

**CO₂ gasification of industrial cokes and characterization of cokes
produced in laboratory**

By

Sania Tasnim Basher

A thesis submitted in partial fulfillment of the requirements for the degree of

Master of Science

in

Chemical Engineering

Department of Chemical and Materials Engineering

University of Alberta

© Sania Tasnim Basher, 2017

ABSTRACT

Metallurgical coke is an important raw material for iron making in a blast furnace. Two significant criteria for selecting high quality coke are Coke Reactivity Index (CRI) and Coke Strength after Reaction with carbon dioxide (CSR). CSR and CRI tests are expensive, labor-intensive and time-consuming. Meanwhile, CSR has linear inverse relation with CRI. Hence, research for coke quality can be focused on coke reactivity with CO₂, which depicts the CRI. Part of this study aims at analyzing coke gasification with carbon dioxide of industrially manufactured coke. Thermogravimetric analysis of cokes was conducted by heating the cokes to a certain temperature and soaking in CO₂. Using non-isothermal methods, the kinetic parameters, such as activation energy and pre-exponential constant, were calculated during the heating period in CO₂. Conversions during the soaking period were also obtained from TGA and were correlated with CRI of the cokes. Another part of study was concentrated on production of cokes in laboratory. Different bituminous, coking coals and a sub-bituminous coal were used for coal carbonization, which was conducted in a horizontal tube furnace by heating samples in an inert atmosphere at different heating rates. Samples were also produced by addition of two binders, asphaltene and ash free coal, in bituminous and sub-bituminous coal and the effect of the binders on the carbonization products were studied. In this study, the CO₂ reactivity of the cokes was detected by using Thermogravimetric Analysis (TGA); the samples were heated to 1100°C in an inert atmosphere and soaked at 1100 °C in CO₂ for two hours. Total porosity of the cokes was determined by using image stitching of thin sections in digital microscopy at 250X magnification, followed by image processing in MATLAB. Raman spectroscopy was carried out to observe the spectra radiated from the coke samples, which gave two distinct peaks, indicative of graphitic carbon and disoriented carbon; extent of graphitization was calculated using the area under the peaks.

Keywords: *coke, CRI, kinetic parameters, carbonization, binder, conversion, porosity, Raman spectroscopy*

PREFACE

Some of the researches conducted for this thesis is part of MITACs accelerate research project with Teck Metals Ltd. (led by Qun Zhang) and University of Alberta (led by Professor Dr. R. Gupta). The technical apparatus referred in Chapter 3 was designed and modified by myself with the assistance of Dr. D. Pudasainee and Dr. R. Gupta. The data analyses in chapter 4, the conclusive analysis in chapter 5 along with the literature review of chapter 2 are originally my work. One of the binders, ash free coal, used in this study was part of research in the following paper.

- Rahman, M., Samanta, A., & Gupta, R. (2013). Production and characterization of ash-free coal from low-rank Canadian coal by solvent extraction. *Fuel Processing Technology*, 115, 88–98.

ACKNOWLEDGEMENTS

When I started my Master's Program at University of Alberta, I had minimal knowledge in the area of this study and I am really grateful to each and every person who had major contribution and impact on towards my research.

First of all, I would like to express my respectful gratitude to my supervisor, Dr. Rajender Gupta for his encouragement, sincere guidance and support throughout the years. Additionally, I would like to extend my thanks to all of my wonderful group members who helped me in each and every step during my research. I am very grateful to our Post Doctorate fellow, Dr. Deepak Pudasainee for always being there, for training me with the instruments, for his timely suggestions and for constructive remarks towards upgrading my work. I would also like to thank Dr. Mehdi Mohammadalipour for teaching me Raman Spectroscopy and image processing. I am thankful to Dr. Vinoj Kurian for time to time advices, regarding my work. Thanks to Keji Wan for helping me learn OriginPro; that has been a major help. Thanks to Monir Khan for providing some background information for my work. I am grateful to Nisarg Tripathi for motivating me to note down important findings from the research papers in a notebook; this has helped me a lot for compilation of the literature review. Thank you, Ananthan Santhankrishnan, for offering help during my experiments and also for reminding me, always, to race with time! A special thanks to Madhumita Patel for her analytical helps, wise advices and inspiring, optimistic words every time I have been stressed out.

I am grateful to James McKinnon from CME machine shop for making the steel crucibles for my experiments. Thanks to Martin von Dollen and Mark Labbe for helping with all my thin section

samples. Heartiest thanks to the CMEGSA 2016-2017 committee for organising the MATLAB workshop which enhanced my knowledge for using that software in my research work.

Last but not the least, I would like to extend my appreciations to my family and friends whose inspirations helped me go forward and especially to my husband, Soiket, for supporting me throughout this journey.

This research was made possible through the financial contribution of Teck Metals and technical contribution of Dr. Qun Zhang from Teck Metals. I am highly indebted to Mitacs Accelerate Program for contributing in this research.

TABLE OF CONTENTS

ABSTRACT.....	ii
PREFACE.....	iv
ACKNOWLEDGEMENTS.....	v
LIST OF TABLES.....	x
LIST OF FIGURES.....	xii
1. INTRODUCTION.....	1
1.1. Coal overview:.....	1
1.1.1. Global demand.....	2
1.2. Importance of Coke in Iron Making.....	3
1.3. Motivation.....	4
1.4. Source of coal and coke.....	5
1.5. Thesis outline.....	5
1.6. Research objectives.....	7
2. LITERATURE REVIEW.....	8
2.1. Role of coke in blast furnace.....	8
2.2. Important features of metallurgical coke.....	8
2.2.1. Coke Reactivity Index (CRI).....	9
2.2.1.1. Factors affecting CRI.....	10
2.2.2. Coke Strength after Reaction (CSR).....	10
2.3. Coke Manufacturing.....	12
2.3.1. Fundamentals of Coal Carbonisation and Coke Formation.....	12
2.3.2. Manufacturing process.....	12
2.4. Coke gasification behavior with carbon dioxide.....	15
2.4.1. Direct Arrhenius method.....	16
2.5. Laboratory scale production of coke.....	18
2.6. Addition of binders in coke.....	24
2.6.1. Use of ash free coal as binder.....	25
2.6.2. Use of asphaltene as binder.....	26
3. EXPERIMENTAL PROCEDURE.....	27

3.1	Materials.....	27
3.2	Sample preparation for coal carbonization in horizontal tube furnace	28
3.2.1	Coal samples.....	28
3.2.2	Coal samples with binders.....	28
3.3	Experimental set-up.....	29
3.4	Experimental procedure	31
3.5.1	Ash analysis.....	32
3.5.2	Thermo-gravimetric analysis with CO ₂	33
3.5.3	Optical microscopy.....	34
3.5.4	Raman spectroscopy.....	36
4.	RESULTS AND DISCUSSIONS-I Coke gasification with carbon dioxide.....	37
4.1.	Mass and derivative mass Vs Time plots.....	37
4.2.	Activation energy and pre-exponential constant.....	40
4.3.	Conversion factor during soaking period and CRI.....	42
4.4	Conclusions.....	43
5.	RESULTS AND DISCUSSIONS- II Characterization of cokes prepared in horizontal tube furnace.....	45
5.1.	Effect of heating rate during de-volatilization on coking	45
5.1.1.	Coking yield	45
5.1.2.	Ash analysis.....	46
5.1.3.	CO ₂ gasification.....	46
5.1.4.	Image analysis of coke	48
5.1.5.	Extent of graphitization	50
5.2.	Effect of addition of binders.....	52
5.2.1.	Effect of addition of asphaltene.....	52
5.2.1.1.	Ash Analysis	52
5.2.1.2.	CO ₂ gasification	53
5.2.1.3.	Image analysis of coke.....	55
5.2.1.4.	Extent of graphitization.....	58
5.2.2.	Effect of ash free coal addition.....	60
5.2.2.1.	Ash analysis	60

5.2.2.2.	CO ₂ gasification	61
5.2.2.3.	Image analysis of coke.....	63
5.2.2.4.	Extent of graphitization.....	65
5.3.	Conclusions	68
6.	CONCLUSIONS AND FUTURE WORK.....	70
6.1.	Conclusions	70
6.2.	Future Work	71
	BIBLIOGRAPHY	72
	APPENDICES	80
	Operation of the horizontal tube furnace	80
	Steps of image processing to find total porosity of cokes	82
	Steps of calculation for extent of graphitization	82

LIST OF TABLES

Table 1.1 Major coking coal Exporters (Mt)	4
Table 3.1 Properties of parent coals and the industrially produced cokes	27
Table 3.2 Summary of samples with addition of binders	29
Table 4.1 Activation Energy, Pre-exponential constant, Correlation coefficient of four coke samples using Direct Arrhenius Method.....	41
Table 4.2 Comparison of literature data and experimental data for Direct Arrhenius	42
Table 4.3 Conversion during soaking period at 1100°C and CRI of the cokes	43
Table 5.1 Effect of heating rate on coking yield.....	45
Table 5.2 Effect of heating rate on ash content of cokes	46
Table 5.3 Effect of heating rate on conversion in CO ₂ at 1100 °C	47
Table 5.4 Effect of heating rate during de-volatilization on total porosity (%).....	49
Table 5.5 Effect of heating rate during de-volatilization period on extent of graphitization of cokes	51
Table 5.6 Effect of asphaltene on ash content of cokes	52
Table 5.7 Effect of asphaltene addition on conversion during the isothermal period in CO ₂ and total mass loss	54
Table 5.8 Effect of asphaltene addition on total porosity (%) of coke samples	56
Table 5.9 Area under Ad, Ag and extent of graphitization for the samples	59
Table 5.10 Effect of ash free coal on ash content of cokes.....	60

Table 5.11 Effect of ash free coal addition on conversion during isothermal period in CO ₂ and total mass loss	62
Table 5.12 Effect of ash free coal addition on total porosity (%) of cokes	64
Table 5.13 Effect of ash free coal addition on Ad, Ag and extent of graphitization for the samples	67

LIST OF FIGURES

Figure 1.1 Total primary energy supply in 2015	2
Figure 1.2 World coking coal consumption (Mt)	3
Figure 2.1 Relation between CSR and CRI of coke	11
Figure 2.2 Beehive oven for coke making	13
Figure 2.3 Cross-sectional view of recovery and non-recovery coke ovens	15
Figure 2.4 Direct Arrhenius plot for calculation of kinetic parameters, E and A.....	17
Figure 2.5 Electrically heated coke test oven	19
Figure 2.6 Schematic Diagram of Jenkner's Retort.....	21
Figure 2.7 Sole-heated oven for semi-coke formation	23
Figure 3.1 Horizontal Tube Furnace used for coal carbonization	30
Figure 3.2 Schematic Diagram of Experimental Set-up.....	31
Figure 3.3 Thermo-Gravimetric Analyzer used.....	33
Figure 3.4 Keyence automated microscope used for image analysis	35
Figure 3.5 Raman spectrometer used.....	36
Figure 4.1 Mass Vs time plot (Method I)	37
Figure 4.2 Derivative mass vs time plot (Method I).....	38
Figure 4.3 Mass loss Vs time plot (Method II).....	39
Figure 4.4 Derivative mass loss Vs time plot (Method II)	39

Figure 4.5 Arrhenius plot for Ck3.....	40
Figure 4.6 CRI plotted against conversion factor at soaking period.....	43
Figure 5.1 Effect of heating rate on conversion in CO ₂ at 1100 °C.....	47
Figure 5.2 Stitched image of MCX at a) 5 °C /min and b) 2.5 °C /min (250X)	48
Figure 5.3 Effect of heating rate during de-volatilization on total porosity (%)	49
Figure 5.4 Raman Spectrum of DC.....	50
Figure 5.5 Effect of heating rate during de-volatilization period on extent of graphitization	51
Figure 5.6 Effect of asphaltene on ash content of cokes.....	53
Figure 5.7 Effect of asphaltene addition on conversion during isothermal period.....	54
Figure 5.8 Stitched image of a) pure DC b) DC10Asp c) DC20Asp d) DC10AFC10Asp (250X)	56
Figure 5.9 Effect of asphaltene addition on total porosity (%).....	57
Figure 5.10 Raman Spectrum of DCR.....	58
Figure 5.11 Effect of asphaltene addition on extent of graphitization.....	59
Figure 5.12 Effect of ash free coal on ash content of cokes	61
Figure 5.13 Effect of ash free coal addition on conversion during isothermal period.....	62
Figure 5.14 Stitched image of a) pure DC b) DC10AFC c) DC20AFC d) DC10AFC10Asp (250X)	64
Figure 5.15 Effect of ash free coal addition on total porosity (%)	65
Figure 5.16 Raman Spectrum of DCR.....	66

Figure 5.17 Effect of ash free coal addition on Extent of graphitization..... 67

1. INTRODUCTION

1.1.Coal overview:

Coal is a naturally occurring carbonaceous matter that is formed from plant matters buried over long period of time. Micro-structural examination of coal reveals fossil imprints of vegetal matter such as leaf, bark and other components of tree and it also implies that formation of coal took place from fossilisation of plants. Coal forms in two steps, namely biochemical period and dynamo-chemical period. During the biochemical period, the plant matter buried under the soil decomposes by action of bacteria in presence of moisture and air and forms a partially decayed plant matter known as peat. During the dynamo-chemical period, layers of peat go through chemical and physical changes due to changing pressure and temperature of earth's crust throughout the years. Pressure and temperature causes continual chemical changes in carbonaceous matter in peat and it gradually transforms into coal.

Coal can be classified into lignite, sub-bituminous, bituminous, semi-anthracite and anthracite based on the degree of transformation of peat to coal. Anthracite is of highest rank and lignite is of lowest [Saxena & Tiwari, 2016]. The coals of high rank are suitable for use as metallurgical coal to produce coke. The other coals, having high calorific values as well, are widely used as fuel is known as thermal coal [Gupta, 2008].

Coke is a black, porous, complex, carbon-rich matter which is obtained from coal. Metallurgical coke is one of the core ingredients for steel-making.

1.1.1. Global demand

Coal is one of the largest sources of global energy and it provides around one-third of world's primary energy, according to the International Energy Agency report, as shown in Figure 1.1.

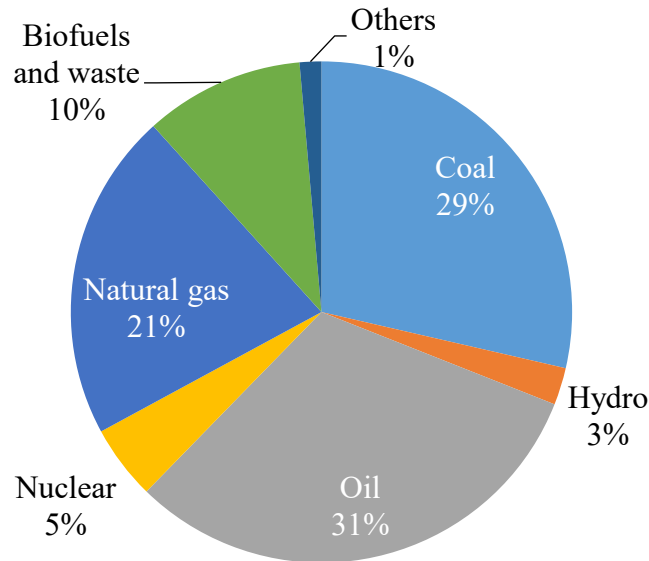


Figure 1.1 Total primary energy supply in 2015

However, due to massive amount of emissions of greenhouse gases by combustion of coal and its adverse effect on extreme climate change, G7 leaders insisted on phasing out fossil fuel, including coal by 2100 [Connolly & Kate, 2015]. Hence, the coal-fired power plants are under pressure to be shut down or else to continue through clean coal technology.

On the other hand, there is a rapid increase in global pig iron production. [<http://www.bhp.com>]. Hence, there is also high demand of metallurgical coal for production of coke. According to International Energy Agency, within 2013 to 2015, coking coal trade around the world had increased by 5 Million tonnes. The increasing trend of coking coal consumption from 1978 to 2015 is shown in Figure 1.2.

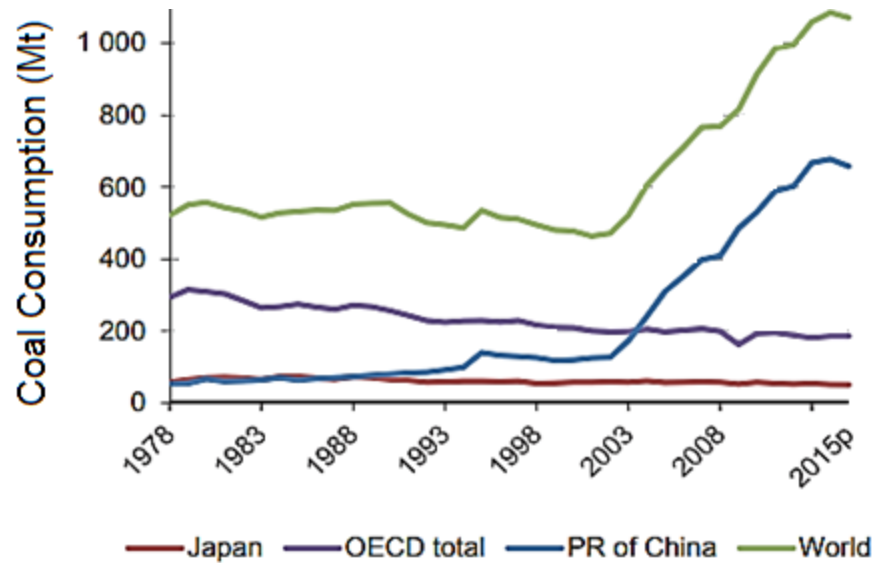


Figure 1.2 World coking coal consumption (Mt) [EIA, 2016]

1.2.Importance of Coke in Iron Making

Coke is one of the main raw materials for production of iron. It has several roles in the blast furnace. It acts as a reducing agent for reduction of iron ore to iron. It acts as a fuel for providing energy for melting the charge and also for the reactions. More importantly, the alternate layers of coke, iron ore and limestone charged in the furnace it provides support of the burden as well as a permeable bed for the gaseous products. The first two roles can be replaced by other materials such as oil, gas, plastics and coal but the final role as permeable bed makes coke an indispensable raw material for iron making [Diez, 2002]. For every 1400kg of iron ore in blast furnace, around 800kg of coal is required [Worldsteel, 2012].

1.3.Motivation

Table 1.1 Major coking coal Exporters (Mt) [IEA, 2016]

<i>Country</i>	<i>2013</i>	<i>2014</i>	<i>2015p</i>
<i>Australia</i>	154.2	180.5	187.7
<i>United States</i>	59.6	54.5	41.7
<i>Canada</i>	35.0	31.1	28.0
<i>Russian Federation</i>	21.5	21.1	18.3
<i>Mongolia</i>	7.7	6.0	7.7
<i>Other</i>	16.7	17.5	15.6
<i>World</i>	294.9	310.7	299.2

Metallurgical coke is an important raw material for iron production. The global coking coal exports from 2013 to 2015 are as shown in Table 1.1. Canada is the third major coking coal exporters of the world. According to researches, use of high quality coking coals leads to improved quality of coke and this in turn, increases productivity of blast furnace performance for iron making [Diez, 2002]. Hence, this calls for lots of research in coking coals and cokes. Moreover, due to limited resources of metallurgical coal reserves in the world, there have been researches for coal blending with additives and/or thermal coal to study their potential in blast furnace [Krezesinska, 2010] [Diez, 2002].

1.4. Source of coal and coke

The metallurgical coals and cokes used in this research originate from the mines in British Columbia. The thermal coal used in this study was obtained from mine in Alberta. The asphaltene which has been used as a binder was collected from by-product of oil-sand mine in Northern Alberta. The source of coal used to prepare ash-free coal, as binder, was mined from Western Canada too.

1.5. Thesis outline

For ease of understanding, this thesis has been segmented into five chapters. The content of each chapter is as discussed in brief below.

The first chapter comprises of the overview of coal and global demand and importance of coke in iron making. This chapter also includes the motivation for this research and the research objectives.

The second chapter elaborates on metallurgical coke, its roles in blast furnace and important features of coke, along with the factors affecting them. Alongside, the theory behind coal carbonisation and coke formation during coke manufacturing are discussed. Theories regarding kinetic study of coke gasification with carbon dioxide have been covered. Some of the researches related to lab-scale production of coke are included too. Lastly, researches related to addition of binders in coke have been mentioned.

The third chapter includes the details of experimental setup design. Apart from that, this chapter also features the details of characterisation techniques used in this study.

The fourth chapter includes the coke gasification with carbon dioxide, calculation of activation energy, pre-exponential constants and conversion.

The fifth chapter includes results of characterization of cokes carbonized in horizontal tube furnace with addition of asphaltene and ash free coal.

The final chapter (Chapter 6) contains the conclusions from this study along with suggestions for future research works.

The working procedure of the horizontal tube furnace, the steps for image processing and the steps of calculation for extent of graphitization are presented in the Appendices.

1.6. Research objectives

The quality of any metallurgical coke is judged by Coke Reactivity Index (CRI), and Coke Strength after Reaction (CSR). There is a nearly linear inverse relation between CRI and CSR i.e. higher the Coke Reactivity Index lower is the CSR. Hence it is crucial to understand the gasification behavior of different cokes with carbon dioxide. The first segment of this study is focused on the kinetic study of several industrially produced cokes. Rest part of this research was to carbonize coal in laboratory and it necessitated the design of a lab-scale horizontal tube furnace so as to carry out coal carbonisation. The objectives of this research are as follows:

1. TGA as an alternate method for CRI tests
 - To study CO₂ gasification of industrially manufactured cokes
2. Effect of additive in coals on coke prepared in horizontal furnace
 - To gain better understanding on effect of de-volatilization time and soaking time on product
 - To study the effect of ash free coal addition in coke properties
 - To study the effect of asphaltene addition in coke properties

2. LITERATURE REVIEW

2.1.Role of coke in blast furnace

Coke is one of the three main raw materials used in blast furnace for iron making. During iron making, iron ore, limestone and coke are alternately charged inside the furnace. Coke has several important roles in the blast furnace during coke making. Thermal role of the coke is to act as a fuel for the chemical reactions to take place inside the furnace. As chemical role, coke acts as a reducing agent for reduction of iron ore to iron. It also has physical roles, i.e. it acts as a permeable bed for gas flows within the furnace and it also provides strength for sustaining the burden of the raw materials [Hilding, 2005]. Therefore, it is very crucial to select appropriate coke for blast furnace as it is undesirable to have the coke degraded quickly. There are several causes of coke degradation that needs to be considered before selection of coke. Stress accumulations inside blast furnace and coke properties are to name a few. Accumulation of stress is required to be controlled while operating the furnace, however, coke properties can be taken into account beforehand. Therefore, it is essential to know certain coke properties before selection [Hilding, 2005].

2.2.Important features of metallurgical coke

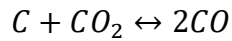
There are several quality requirements of a metallurgical coke. They are mentioned briefly below.

- i) Chemical composition (such as fixed carbon, amount of ash, mineral content)
- ii) Reactivity with different gaseous products inside the furnace
- iii) Particle size range
- iv) Thermal stability at elevated temperature
- v) Strength and abrasion resistance [Tupkary and Tupkary, 2013].

Two of the important properties of coke are namely Coke Reactivity Index (CRI) and Coke Strength after Reaction (CSR).

2.2.1. Coke Reactivity Index (CRI)

Coke reacts with carbon dioxide to form carbon monoxide, with following reaction.



This is an undesired and yet, inevitable reaction occurring in the furnace. Loss of mass due to this reaction causes coke degradation. Overall, this reaction is detrimental for operation of furnace [Tupkary and Tupkary, 2013].

Coke Reactivity Index can be defined as the amount of mass loss upon exposure of coke to carbon dioxide atmosphere at elevated temperature for designated time period (2 hr). The ASTM standard method for determining CRI is as described below.

200g sample of (-22.4 + 19.0 mm size range) coke is heated up to 1100°C in an inert atmosphere like Nitrogen, Argon etc. After reaching 1100°C, the inert gas flow is stopped and carbon dioxide is passed through the sample for two hours, maintaining isothermal condition [ASTM D5341].

The CRI is then determined from the following equation:

$$CRI = \frac{200 - \text{remaining mass}}{200} \times 100$$

2.2.1.1. Factors affecting CRI

The following factors are responsible for determining CRI of a coke.

- Chemical structure: Greater the number of active sites of carbon, greater will be the reactivity of the coke with carbon dioxide and higher will be the CRI [Fuertes, 1989] [Sato, 1998] [Willmers, 1992].
- Physical structure: Greater the surface area and higher the amount of pore, greater will be the rate of reaction and control of diffusion. Thus, higher will be the CRI [Fuertes,1989] [Sato, 1998] [Willmers, 1992].
- Inorganic constituents of coke: Presence of certain minerals in parent coal such as iron containing minerals may induce catalytic graphitization reaction at lower temperature (750-850°C) than graphitization that usually occurs at 950°C. Thus, reaction rate and CRI of coke will be higher when larger amount of those minerals are present in the parent coal [Fuertes, 1989] [Sato, 1998] [Willmers, 1992].

2.2.2. Coke Strength after Reaction (CSR)

Coke strength after reaction (CSR) is another essential feature of coke. The ASTM standard method for obtaining CSR of a coke is as described below.

This test is done simultaneously with the CRI test. The amount of mass obtained after reaction with carbon dioxide at 1100°C for two hours (remaining mass) is taken into a tumbler and rotated at 20rpm for 30 minutes. After the 600th revolution, the samples are subjected to sieving using mesh size of 9.5 mm. The particles that lie below this size i.e. (-9.5) mm are discarded and the

(+9.5) mm fractions are used for determining the CSR using the following equation [ASTM D5341].

$$CSR = \frac{(+9.5)mm \text{ fractions}}{\text{Remaining mass}} \times 100$$

It has been observed that when the CSR of a coke is high, there is a lower chance of the coke to break down, higher permeability for gas and liquids and the coke is more cost-effective due to lower coke consumption [Grosspietsih, 2000].

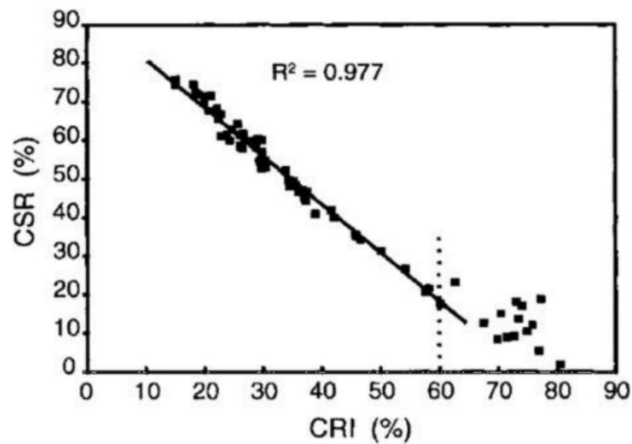


Figure 2.1 Relation between CSR and CRI of coke [Rodero, 2015]

There have been lots of research to correlate these two important features of coke i.e. CRI and CSR and it has been observed that there is a linear inverse relationship between CSR and CRI as shown in Figure 2.1. As can be observed in above figure, when the CRI of a coke sample is high, the CSR of the same will be low [Rodero, 2015].

2.3 Coke Manufacturing

2.3.1 Fundamentals of Coal Carbonisation and Coke Formation

When coal is heated in inert atmosphere, several changes take place in the coal. There are mainly three stages of coal carbonization, namely pre-plastic stage, plastic stage and post-plastic stage. Pre-plastic stage is considered the stage below 350°C. During this stage, moisture gets released from coal and some mass loss takes place. Carbon dioxide is also evolved from light hydrocarbons. At temperature above 200°C, volatile matter starts evolving. During the plastic stage, this is between 350°C and 500°C, molecules break down and rapid evolution of volatile matter takes place. At around 500°C, the glassy phases of mineral content present in coal softens and coal becomes plastic. During the post-plastic stage, Hydrogen is removed from the organic compounds by condensation and more ordered structure formation takes place. At around 600°C, it transforms into black porous macrostructure of semi-coke. The evolution of these volatile matters may continue up to temperature as high as 750°C and finally grey, solid mass of coke formation takes place. In terms of chemical changes in coal during carbonization, pyrolysis of coal also takes place and the organic structures may undergo cracking reaction or aromatization. Cracking gives rise to the liquid products which re-solidify when aromatization takes place [Sivanaskar, 2008] [R. Loison, 1989] [Diaz-Faes, 2007].

2.3.2 Manufacturing process

During nineteenth and early of twentieth century, manufacturing of coke had been carried out using beehive oven. The oven had a dome shaped top with a door at the top through which coal was charged. Discharging door was bricked during the carbonization method. When coke

formation was complete, the door was broken and coke was taken out [Belden, 1913]. The coke production in the simple beehive oven was time consuming and there was no recovery of by-products [Burger and John,1979]. A cross-section of the bee-hive oven is shown in Figure 2.2.

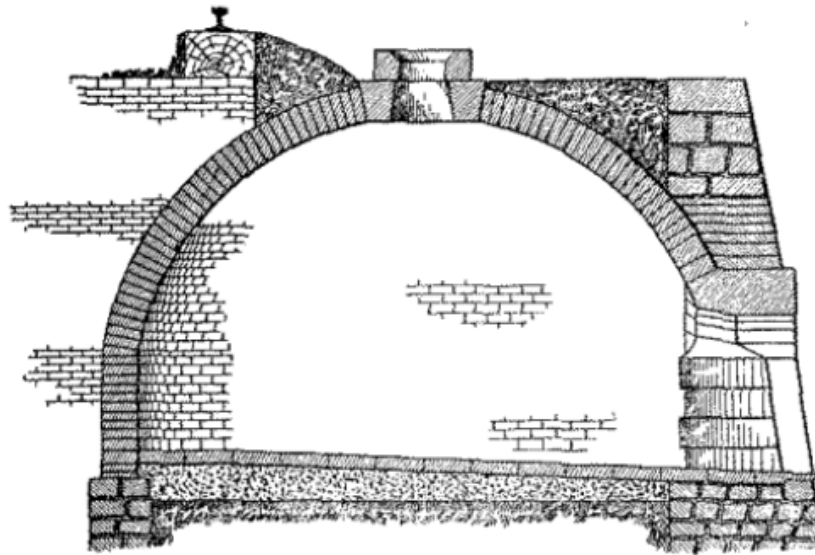


Figure 2.2 Beehive oven for coke making [Belden, 1913]

A widely used method for production of coke is the Otto Hoffman method using a chamber oven or a by-product oven. Coke production process by this method has a higher thermal efficiency as the different by-products of the coke such as coal tar, ammonia, sulphur and coke oven gas are recovered [Sivanaskar, 2008]. These kind of recovery ovens are usually tall and narrow and are used in groups (of 10-100) called batteries. Coal charge is continuously heated at a constant rate by use of a secondary fuel such as blast furnace gas, coke oven gas etc. in presence of high pressure [Saxena & Tiwari, 2016]. This technology however has a major drawback of air pollution by gas leakage through the door [Bermudez, 2013].

Non-recovery coke-making technology is also widely used for manufacturing of metallurgical coke. These are modified beehive ovens which are also operated in batteries. Coal charge is heated by burning volatile matter inside the oven chamber and also by sole heating flues. Carbonisation of coal takes place from the top surface by radiation and conduction while the bottom side is carbonised by conduction of the sole flue. Initially as the coal is fed into the hot chamber, coal ignites at the surface and release volatile matter. This volatile content is burned by controlled airflow and causes carbonisation by heating at the top. This coal carbonisation progresses from the top to the bottom. At the same time, the carbonisation due to heating of chamber floor by sole flue progresses towards the top surface. The carbonisation rate from top and bottom can be optimised by controlling the primary and secondary airflows and thus, improving coke quality. This non-recovery method uses negative pressure and the hydrocarbons are burned within the chamber itself, reducing possibility of air pollution through leakage. The operational cost is also low [Knoerzer and Cekela, 1993]. Cross-sectional view of a recovery and non-recovery coke oven is as shown below in Figure 2.3.

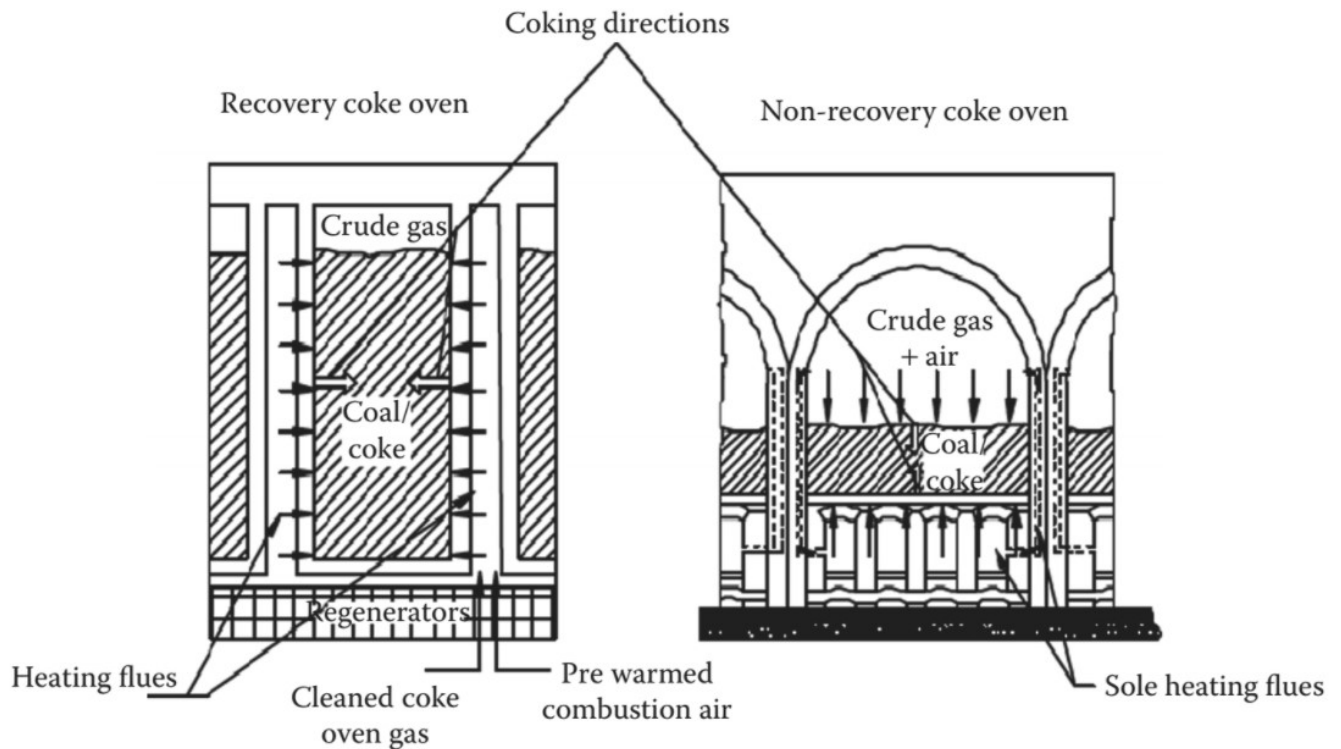


Figure 2.3 Cross-sectional view of recovery and non-recovery coke ovens

[Saxena & Tiwari, 2016]

2.4 Coke gasification behavior with carbon dioxide

Lots of researches have been going on regarding the coke gasification behavior with carbon dioxide. In laboratory, coke gasification with carbon dioxide is often studied through Thermo-Gravimetric Analysis. For Thermo-Gravimetric Analysis, two kinds of properties are mainly focused on:

- 1) The kinetic parameters such as rate constant, activation energy of the reaction, pre-exponential constant
- 2) Reactivity of the coke with carbon dioxide at a certain temperature for a certain period of time

The kinetic parameters can be calculated from non-isothermal methods such as Direct Arrhenius Method, Coats & Redfern Method, shrinking core model etc. One of these methods are discussed below.

2.4.1 Direct Arrhenius method

The rate of mass loss due to gasification is given by the following equation:

$$\frac{dm}{dt} = k \cdot m \quad (1)$$

for a first order reaction, where m is the mass of reactant at any time t and k is the gasification rate constant.

The rate constant k is expressed by Arrhenius Equation as given below.

$$k = Ae^{-E/RT} \quad (2)$$

Where, A is the pre-exponential factor, E is the activation energy in J/mol, R is the universal gas constant i.e. 8.314J/K mol and T is Temperature in K.

If a dimensionless mass fraction, α , is consumed and $(1-\alpha)$ is the mass fraction of total combustible mass, $(m_i - m_f)$, present at time t where, m_i = initial mass, m_T = instantaneous mass at temperature, T , m_f = final mass at end of reaction, then, conversion factor,

$$\frac{(m_i - m_T)}{(m_i - m_f)} \text{ Such that } 0 \leq \alpha \leq 1 \quad (3)$$

Equation (1) can be converted to equation (4) for an n th order reaction.

$$\frac{d\alpha}{dt} = k(1 - \alpha)^n \quad (4)$$

For a first order reaction, $n=1$ and it can be shown that

$$\frac{1}{1 - \alpha} \frac{d\alpha}{dt} = Ae^{-E/RT} \quad (5)$$

Taking natural logarithm, \ln , on both sides of (3),

$$\ln \left[\frac{1}{1 - \alpha} \frac{d\alpha}{dt} \right] = \ln(A) - \frac{E}{RT} \quad (6)$$

Considering the above equation as $y=mx +c$, where $y= \ln \left[\frac{1}{1 - \alpha} \frac{d\alpha}{dt} \right]$, $m= -\frac{E}{R}$, $x = \frac{1}{T}$ and $c = \ln(A)$, a series of TGA data can be plotted using Equation (4) with $\ln \left[\frac{1}{1 - \alpha} \frac{d\alpha}{dt} \right]$ Versus $\frac{1}{T}$ to yield a more or less straight line, the slope of which gives $-\frac{E}{R}$ and intercept will give $\ln(A)$ [Urych, 2014] as shown in Figure 2.4.

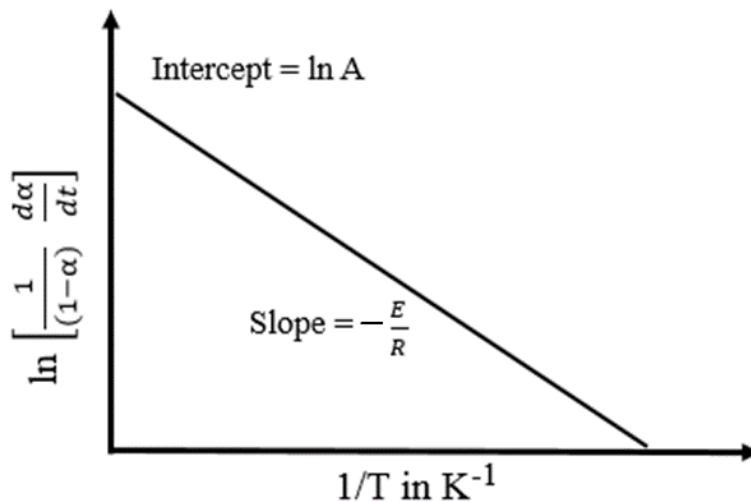


Figure 2.4 Direct Arrhenius plot for calculation of kinetic parameters, E and A

Conversion factor during a certain period is calculated using the following formula,

$$\alpha = \frac{m_{i,t_i} - m_{f,t_f}}{m_{i,t_i} - m_{ash}}$$

Where

m_{i,t_i} = mass of sample at initial time, t_i

m_{f,t_f} = mass of sample after a certain period of time, t_f

m_{ash} = mass of ash in the sample

2.5 Laboratory scale production of coke

Many researches have been progressed in to producing coke in the laboratory. Researchers have tried different procedures, working temperature and different furnaces for producing coke. Some of the researches are as discussed briefly.

Hays et al., [Hays, 1976] had performed carbonisation of coal in sole-heated oven with vertically heated walls. 400gm of coal was air-dried and stacked into an asbestos-paper box of dimensions (70x70x90mm) with a packing density of around 820kg/m³. Coals used in this test were of average particle size more than 1mm and around 12% of the particles were finer than 0.12mm. The asbestos-paper box containing the sample was held in a steel-asbestos box and inserted into the oven. Silicon-coated thermocouples were placed inside the coal charge. The box was purged with pure nitrogen while being heated at 3 °C /min. The box was taken out from heating when the lowest temperature in one of the thermocouple showed 300 °C and the highest temperature was approximately 1100 °C. The box was then allowed to cool naturally.

Okuhara et al., [Okuhara, 1981] had carbonised coal in an electrically heated oven with Silicon Carbide wall with dimensions of 400mm width, 680mm length and 459mm height. They had taken 70kg of coal for carbonisation. The carbonisation temperature was 1100°C. After carbonisation, the cokes were cooled by water spray. The schematic diagram for his test oven is as shown in Figure 2.6.

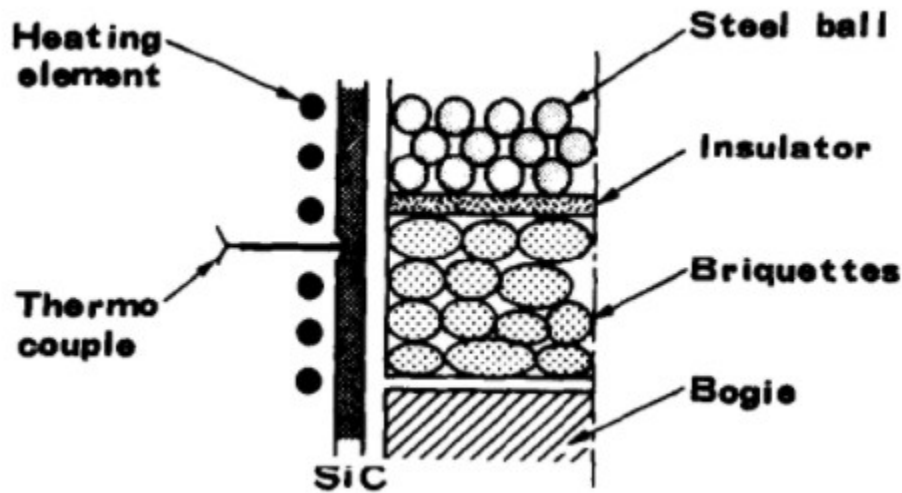


Figure 2.5 Electrically heated coke test oven [Okuhara, 1981]

Grigore et al. [Grigore, 2006] had produced coke in an electrical furnace with a capacity of 9 kilograms. They used coal particles of average size less than 6mm packed into a cylindrical retort with a packing density of 850 kg/m³. Temperature of the furnace was raised to 1050°C before inserting the retort into it. When the centre of the coal charge reached 900°C, it was kept for 50 minutes to let the central temperature rise to 1050°C. The charge was kept inside the furnace for 3hrs in total and then cooled down in Nitrogen atmosphere.

Alvarez et al. [Alvarez, 2006] had carbonized coal in semi-industrial scale in a 6 tonne capacity oven of 2.8m height, 0.45m width and 6.5m of length. Coals were stacked in a packing density of $705\pm 25\text{kg/m}^3$. Average flue gas temperature was around 1250°C . Coking was carried out for a total of 18hrs and the products were quenched in water.

Diaz-Faes et al. [Diaz-Faes, 2007] used a movable wall oven with 250kg capacity of dimensions (1m x 1m x 0.456m) for coal carbonisation. The Silicon Carbide wall of the furnace was electrically heated from 800°C to 1130°C with heating rate of 14K/hr. Time was then kept isothermal for 18hrs before product was cooled down to room temperature. Gornostayev et al. [Gornostayev, 2009] performed carbonisation within temperature range of 1065°C and 1090°C . Soaking period was in between 15 hrs 45 min and 16 hrs 30min.

Koszorek et al. [Koszorek, 2009] used coals of less than 3mm particle size, dried them in air and packed into 900kg/m^3 in a Jenkner's Retort. Furnace was heated at around $25^\circ\text{C}/\text{min}$ for up to 800°C and then, the retort was placed inside the furnace. Then heating was continued up to 1000°C and it was kept isothermal for one hr. The retort was then removed from furnace and allowed to cool down to room temperature in 12hrs before disassembling and taking the sample out. A schematic diagram of the Jenkner's retort used in this research is as shown below in Figure 2.7.

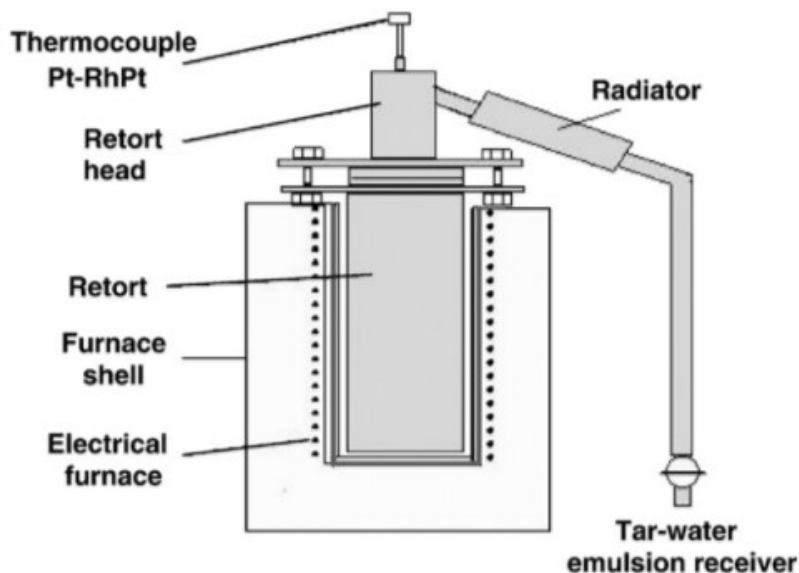


Figure 2.6 Schematic Diagram of Jenkner's Retort [Koszorek, 2009]

Grigore et al. [Grigore, 2012] produced coke in two steps. In the first step, 70g of samples were stacked into a retort with a packing density ranging between 680 to 800 kg/m³. The retort was then inserted into an oven preheated at 300 °C and then heated up to 470 °C at a constant heating rate ranging in between 0.1 °C/min to 1 °C/min with a continuous flow of nitrogen. At 470 °C, the oven was kept isothermal for 2hours and then cooled in nitrogen atmosphere. In the second step, the semi-cokes were placed in an alumina boat and loaded in a horizontal tube furnace. The furnace was heated from ambient temperature to 500 °C with a constant heating rate of 1 °C/min while being purged with high-purity nitrogen gas. The furnace was further heated from 500 °C to 1050 °C at 10 °C/min while it was being purged with high-purity argon gas. During the cooling cycle, the cokes were cooled to 500 °C in an argon atmosphere and from 500 °C to room temperature in nitrogen gas.

Tiwari et al. [Tiwari, 2013] used a carbolite oven of following dimensions: length of 370 mm, width of 115mm and height of 305mm. They used coal particles such that 90% of the particles were smaller than 3.2mm. The coal particles were packed into density of 800kg/m³. Temperature was increased to 1000°C and total time of coking was five hours.

Zhong et al. [Zhong, 2013] used a vertical tube resistance furnace for coke making. 85% of the coal particles were of particle size less than 3mm. 20gm of dry coal was taken into cylindrical metal mould of 90mm diameter and stacked into packing density of 700kg/m³. The furnace was heated at a heating rate of 3°C/min and temperature was increased to 800°C. Nitrogen was purged from the bottom of the furnace at a flow rate of 700mL/s.

MacPhee et al. [Macphee, 2013] produced coke in two steps. First, they made semi-coke in a sole-heated oven of 12kg capacity. The oven was of cubic dimensions with each side of around 280mm. The samples in the oven were pressed from the top with a constant load of around 15kPa. The oven was heated from below by a sole plate whose initial temperature was set at 554 °C and then was heated up to 950 °C. When the top surface of the samples reached 500 °C after around 6-7hrs, the semi-cokes were taken out, quenched in water and dried in an oven at 120 °C. In the next step, the dried semi-cokes of around 9kg were inserted into a stainless steel box. The box was kept inside a muffle furnace and heated to 1100 °C at a heating rate of 5-10 °C/min. Nitrogen gas was continually purged at 5-10mL/min flow rate. The coke was kept isothermal at 1100 °C for 1hr and then cooled to ambient temperature with continued flow of nitrogen. Total time for heating and cooling in this step was around 15hrs. The sole-heated oven used in this coke making is as shown in Figure 2.8.



Figure 2.7 Sole-heated oven for semi-coke formation [MacPhee ,2013]

Mollah et al. [Mollah, 2015] had produced coke in a muffle furnace. They used a mixture of coal and tar for coke making. Coal was dried in Nitrogen atmosphere at 105°C for 24 hrs to reduce moisture content and then, ground to less than 0.15mm. Coal was mixed with tar and moulded into pellets of diameter 13mm and height of 6mm. The pellets were taken into an alumina cup and inserted into the muffle furnace. Nitrogen gas was purged at 400L/hr. Temperature of the furnace was raised to 500°C at a heating rate of 2°C/min. Then, the heating rate was increased to a rate of 5°C/min till the temperature of the furnace reached around 900-950°C. Then, the furnace was kept isothermal at 900°C for 2 to 5hrs. The furnace was cooled overnight with continual flow of Nitrogen.

Nomura et al. [Nomura, 2016] performed carbonisation tests in an electrically heated pilot coke oven with dimensions of 420mm width, 600mm length and 400mm height. Coals were stacked in a steel box with bulk densities ranging from 659 to 830kg/m³. The steel box was inserted into the

coke oven and carbonised for 18.5 hours such that the heating conditions resembled that of an actual coke oven with 1250 °C flue temperature.

Li et al. [Li, 2017] carbonized coal in a quartz reactor placed within an electrical furnace. The temperature was raised to 900°C while being purged with nitrogen of flow rate 0.75L/min. After keeping isothermal at 900 °C for 20 minutes, coal samples were dropped from the top and temperature of 900 °C was maintained for 30 more minutes with continued flow of nitrogen gas. The reactor was then removed from the furnace and the carbonised product was allowed to cool in nitrogen to room temperature.

2.6 Addition of binders in coke

Due to increasing price and deteriorating quality of metallurgical coke around the world, new technologies are necessitated to produce coke with addition of binders in low coking coals [Nomura, 2017]. Many researches have been carried out to use additives with coal to study their effects on the coking properties of the carbonized product.

Wu et al. [Wu, 1968] used coal-tar pitch as a binder. Benk et al. [Benk, 2008] used two types of phenolic resin as binder for making coal briquettes for coke and found that when blend of both of the resins were used, strength of the cokes was increased significantly. Benk et al. [Benk, 2010] had studied the effect of coal tar pitch and phenolic resin on properties of coke and found that when the two binders are added in 1:1 ratio, the strength of the coke increased. Mollah et al. [Mollah, 2015] used tar for binding coal. Silva et al. [Silva, 2016] had used waste tire as a binder in coal and showed that cokes produced from coal-tire mixture showed lower ash content than cokes produced from only coal. He also showed that when waste tire added up to 3%, remarkable CSR values could be obtained in the resulting cokes. Nag et al. [Nag, 2016] had used phenolic

resin for coke making and found that resin improves CSR, Micum 40 Strength (M40), which is the percentage of +40mm size coke after 100 revolutions, and mean size of the cokes.

2.6.1 Use of ash free coal as binder

Ash-free coal, also known widely as hyper-coal, is a derivative of coal that contains minimal amount of ash. Inoue et al. [Inoue, 2008] had used ash-free coal and studied the effect on coke pore distribution and found that ash-free coal increases adhesion of coal particles and reduces gap between the particles. Takanohashi et al. [Takanohashi, 2008] studied effect of ash-free coal addition on coke strength. They found that lower mass loss takes place during coal carbonisation and coke strength increases upon addition of ash-free coal. Hao et al. [Hao, 2012] studied the potential of ash-free coal on caking coals for co-carbonisation of coals. They reached conclusions that addition of small amount of AFC is sufficient for caking coal but large amount is required for weak caking coal. They also found that addition of AFC in weakly caking coal increases adhesion of the coals and make these coals potential feedstock for coke-making. Kim et al. [Kim, 2017] have also used ash-free coal as a binder for coke-making.

Ash-free coal can be produced by solvent extraction of coal. Solvent extraction is carried out in an inert atmosphere in a reactor at high pressure (such as 1MPa) and moderately high temperature (like 350 to 400 °C). While heating, the slurry containing the sample and the solvent are stirred continuously and after about 1 hour, the reactor is cooled to around 100 °C and filtration is carried out using micrometer filters. The residue is then washed repetitively in hexane and finally with acetone. The filtrate is added to a huge volume of a hexane solvent and precipitation of ash-free coal takes place. The precipitated AFC is ready for use after filtration, washing and drying under vacuum [Rahman, 2012].

2.6.2 Use of asphaltene as binder

Asphaltene is a bi-product of oil-sand which has little industrial value. However, these are being used as an additive for coke-making for many researches. McCandless and Blake [McCandless, 1970] used asphaltene as binder in low rank coal for making coke briquettes. They showed that addition of asphaltene reduces mass loss during carbonisation process and briquette strength increases. Paul et al. [Paul, 2002] had also used asphaltene to produce coke briquettes. They found that addition of asphaltene increases the strength of coke briquettes and best result was obtained with more than 20% asphaltene. They also found that briquettes which were cured in air first and then carbonised were of high strength. Trejo et al. [Trejo, 2010] had studied thermo-gravimetric analysis on asphaltene and found that pure asphaltene formed around 47% of coke when heated in inert atmosphere, suggesting the potential of asphaltene as a binder for coking.

3 EXPERIMENTAL PROCEDURE

3.1 Materials

Four Industrially produced cokes, Ck1, Ck2, Ck3, Ck4, four coking coals of bituminous rank, MCX, EC, DC, MCN and one coal of sub-bituminous rank, GC, were used in this study. The properties of coals used are as mentioned in the table below.

Table 3.1 Properties of parent coals and the industrially produced cokes

<i>Coal sample</i>	<i>Moisture content (%)</i>	<i>Volatile matter (%)</i>	<i>Fixed carbon db (%)</i>	<i>Ash content db (%)</i>
<i>MCX</i>	0.72	19.19	70.42	10.40
<i>EC</i>	0.70	19.72	67.58	12.70
<i>DC</i>	0.76	19.68	64.93	15.39
<i>MCN</i>	0.86	19.15	70.82	9.87
<i>GC</i>	6.73	34.11	57.9	5.53
<i>Coke sample</i>	<i>Ash content (%)</i>		<i>CRI</i>	<i>CSR</i>
<i>Ck1</i>	11.17		21.6	73.2
<i>Ck2</i>	11.09		22.1	71.5
<i>Ck3</i>	11.18		24.4	66.3
<i>Ck4</i>	11.14		26.1	66

Db: dry basis

CRI: Coke reactivity index

CSR: Coke strength after reaction with CO₂

3.2 Sample preparation for coal carbonization in horizontal tube furnace

Coal samples were carbonized using horizontal tube furnace. Details of the samples and experimental procedure are as follows.

3.2.1 Coal samples

Four metallurgical coal samples, MCX, EC, DC, and MCN and one sub-bituminous coal, GC, were used for preparing coke in horizontal tube furnace. Each sample was crushed using mortar and pestle to -2mm size. The particles less than 0.3mm size were then sieved out from the samples for decreasing bulk density [Sharma, 2007].

3.2.2 Coal samples with binders

One of the three coking coals, DC, and a sub-bituminous coal, GC, were mixed with binder material, i.e. asphaltene and ash-free coal (0% to 20%) to prepare 10 samples. Sample produced from 10% asphaltene and 90% of DC coal has been named DC10Asp and so on.

For preparing the samples, each of the components (coal, ash free coal and asphaltene) was crushed to less than 2mm size and particles less than 0.3mm were sieved out. Then, amount of binder and coal were weighed in desired ratio and mixed well by tumbling. The ten samples carbonized are as mentioned in Table 3.2.

Table 3.2 Summary of samples with addition of binders

<i>Name of Sample</i>	<i>Type of coal</i>	<i>Amount of asphaltene (%)</i>	<i>Amount of ash-free coal (%)</i>	<i>Amount of coal (%)</i>
<i>DC10Asp</i>	Bituminous	10	0	90
<i>GC10Asp</i>	Sub-Bituminous	10	0	90
<i>DC10AFC</i>	Bituminous	0	10	90
<i>GC10AFC</i>	Sub-Bituminous	0	10	90
<i>DC20Asp</i>	Bituminous	20	0	80
<i>GC20Asp</i>	Sub-Bituminous	20	0	80
<i>DC20AFC</i>	Bituminous	0	20	80
<i>GC20AFC</i>	Sub-Bituminous	0	20	80
<i>DC10Asp10AFC</i>	Bituminous	10	10	80
<i>GC10Asp10AFC</i>	Sub-Bituminous	10	10	80

3.3 Experimental set-up

The horizontal tube furnace used for carbonization of the coal samples is as shown in Figure 3.1. The setup consists of a small Thermolyne 79300 tube furnace. The overall furnace unit comprises of a control unit, a tubular heating chamber and a pyrometer. The furnace chamber is heated by metallic coils embedded in a rigid refractory material. The furnace temperature is controlled by the control unit and the temperature is measured by K-type thermocouple in the pyrometer. The electrical connections are placed within the control unit below the furnace chamber. The furnace chamber is a mullite tube with diameter of 59mm and length of 80cm. The quartz tube is sealed at both end and the exposed portion of the tube is insulated using K-wool and Fiberfrax material to minimize heat loss. A primary flow of N₂ gas is used for carbonization of the sample and the gas

flow is adjusted using Cole-Parmer rotameter. Pressure release valve is used at the exit end of furnace to prevent excessive pressure build up within furnace. Volatile matters produced during the experiments are passed through water-based scrubbing solution. A Rocker 300 series pump is used for maintaining unidirectional flow of flue gases. The schematic representation of the experimental setup is as shown in Figure 3.2.



Figure 3.1 Horizontal Tube Furnace used for coal carbonization

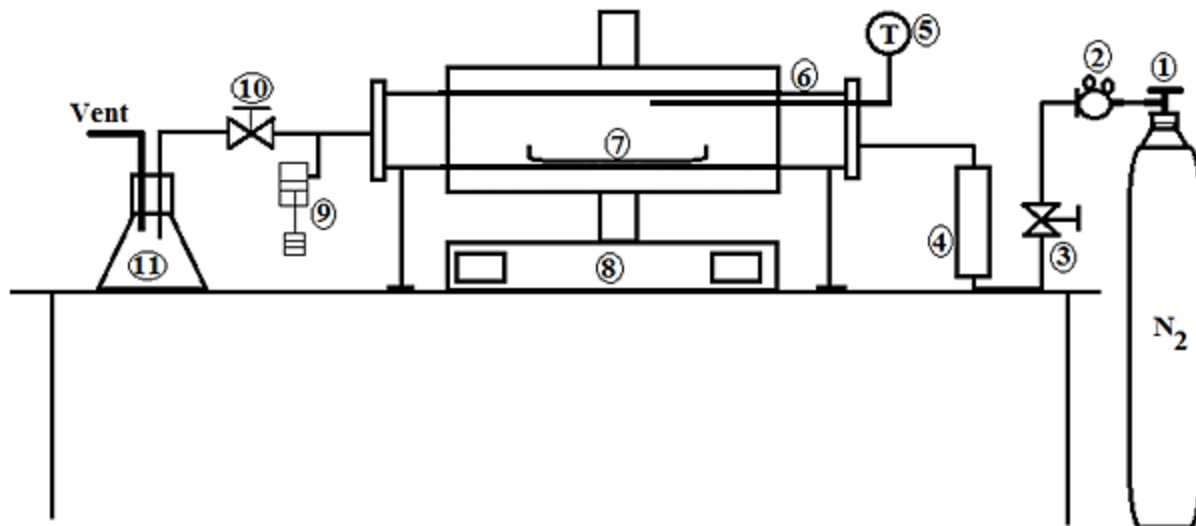


Figure 3.2 Schematic Diagram of Experimental Set-up

- 1) Gas cylinder 2) gas regulator 3) valve 4) rotameter 5) thermocouple 6) Mullite tube 7) sample holder 8) control box 9) pressure release valve 10) valve 11) Scrubbing Solution

3.4 Experimental procedure

Around 7.5gm of coal sample was placed in crucible and placed inside the tube furnace. Before starting the experiment, Nitrogen gas was passed at $10\text{cm}^3/\text{min}$ for 15 minutes to remove any reactive species from the furnace. The furnace was heated at $10^\circ\text{C}/\text{min}$ to 300°C with continuous flow of Nitrogen gas at $10\text{cm}^3/\text{min}$. Then, for effective de-volatilization of volatile content of coal, heating rate was decreased to $5^\circ\text{C}/\text{min}$ up to 500°C with increased Nitrogen flow of $25\text{cm}^3/\text{min}$. After reaching 500°C , the heating rate was increased back to $10^\circ\text{C}/\text{min}$ with decreased Nitrogen flow of $10\text{mL}/\text{min}$ until temperature reached 900°C . Then, at 900°C , sample was held isothermally for 6 hours. The furnace was then cooled at $2^\circ\text{C}/\text{min}$ with continued flow of Nitrogen.

A second set of experiments was carried out using a lower heating rate i.e. 2.5°C/min during the de-volatilization period of 300°C to 500°C and was followed by 12 hours of soaking at 900°C, instead of 6 hours. The purpose of this (slow heating experiment) was to ensure effective de-volatilization and higher degree of coking.

The experimental procedure was carried out as described below. Around 7.5gm of coal with binder was taken in crucible and placed inside the tube furnace. Before starting the experiment, Nitrogen gas was passed at 10cm³/min for 15 minutes to remove any reactive species from the furnace. The furnace was heated at 10°C/min to 300°C with continuous flow of Nitrogen gas at 10cm³/min. Then, for effective de-volatilization of volatile content of coal, heating rate was decreased to 2.5°C/min up to 500°C with increased Nitrogen flow of 25cm³/min. After reaching 500°C, the heating rate was increased back to 10°C/min with decreased Nitrogen flow of 10cm³/min until temperature of 900°C had reached. Then, at 900°C, soaking was carried out isothermally for 12 hours. The furnace was then cooled at 2°C/min with continued flow of Nitrogen.

3.5 Characterization techniques

The different characterization techniques used in this study are as discussed below.

3.5.1 Ash analysis

Coal sample was crushed to -0.25mm. About 40mg sample was loaded in alumina crucible. The sample was then heated in air from 25°C to 500°C in 1 hour and from 500°C to 950°C in another 1 hour. Air was flowed at 100cm³/min. Then, it was kept isothermal for 2 hours at 950°C with continued air flow. Using ASTM method (ASTM D3174), ash percent in each sample were calculated from TGA data (SDT DQ600 TA instrument, USA). The ash percentage in the sample was obtained using the following formula.

$$\text{ash \%} = \frac{\text{mass}_{\text{final}}}{\text{mass}_{\text{initial}}} \times 100$$

Where;

$\text{mass}_{\text{initial}}$ is the initial mass of the sample at 25°C

$\text{mass}_{\text{final}}$ is the mass remaining at the end of the experiment at 950°C.

3.5.2 Thermo-gravimetric analysis with CO₂

Thermo-gravimetric analysis (TGA) was carried out using SDT DQ600 TA instrument. The instrument is as shown in Figure 3.3. The analysis was carried out using two different methods as described in the following paragraphs.



Figure 3.3 Thermo-Gravimetric Analyzer used

For calculations of activation energy of the industrially produced coke samples, method I was used. Four different cokes (Ck1, Ck2, Ck3, and Ck4) have been analyzed to study their reactivity with carbon dioxide. The coke samples were crushed to -0.25mm and around 40 mg samples were placed in Alumina pan of TGA. Temperature was ramped at 10°C/min to 1100°C with carbon dioxide flow rate of 100cm³/min. When the temperature reached 1100°C, the samples were kept for two hours with continued flow of carbon dioxide. The mass loss at soak temperatures of 1100°C was also noted for comparison with CRI.

For measuring the reactivity of each sample (the ones produced industrially and those prepared in the laboratory) were subjected to Method II [ASTM D5341]. Sample was crushed to -0.25mm size and around 40mg sample was loaded in alumina crucible. The sample was then heated at 10°C/min up to 1100°C with Nitrogen gas flowing at 100cm³/min. Upon reaching 1100°C, Nitrogen gas was replaced with carbon dioxide and temperature was kept isothermal for two hours. The conversion during the soaking period is calculated on ash free basis, using the formula as given below

$$Conversion = \frac{mass_{1100C,0\ min} - mass_{1100C,120\ min}}{mass_{1100C,0\ min} - mass_{1100C,0\ min} \times mass_{ash} \times 100}$$

Where, $mass_{1100C, 0\ min}$ = mass of sample upon reaching 1100°C
 $mass_{1100C, 120\ min}$ = mass of sample after 120 minutes at 1100°C

3.5.3 Optical microscopy

For preparing slide for optical microscopy, each sample was subjected to vacuum pressure impregnation with blue-dyed resin and a very thin slice (30micron) was cut and mounted on glass. Thin Section slides were mounted on microscope stage and auto-focus was performed by the microscope. Then, at 250X magnification, two-dimensional image-stitching was carried out on

each sample to obtain image of a large area at high resolution. The images were then processed in MATLAB to obtain the porosity of each sample. Keyence VHX-S90BE Automated Microscope was used for obtaining the optical images of the samples. The microscope is as shown in Figure 3.4.



Figure 3.4 Keyence automated microscope used for image analysis

The microscopy images were subjected to threshold (changing to monochromatic or black and white color). Then, total porosity was calculated by using the formula mentioned below. The details of image processing is mentioned in the appendices.

$$Porosity = 100 * A / (A + B)$$

Where,

A = total surface area of the coke sample

B = total surface area of the pores.

3.5.4 Raman spectroscopy

Raman Spectroscopy (SnRI Instrument) was carried out by using polished thin section slides of the samples. The slide was placed inside the chamber, a good location was chosen with least amount of pores and the sample was focused using Toupview software and an in-built camera with low magnification. Laser beam was passed on the sample surface and using Peak software, an average spectrum was obtained from 20 spectra. Two peaks were prominent in each sample, one at around 1300/sec which is the peak for disoriented carbon (D) and the other at around 1600/sec which is of the graphitic carbon (G) [Mennella, 1995]. The Raman Spectrometer is as shown in Figure 3.5.



Figure 3.5 Raman spectrometer used

The peaks obtained from the Raman were used for calculating the extent of graphitization in each sample using the formula mentioned below. The detailed procedure of calculation is briefed in the appendices.

$$\frac{A_g}{A_g + A_d} \times 100 = \text{Extent of graphitization}$$

Where, A_g = Area under G peak and A_d = Area under the D peak

4. RESULTS AND DISCUSSIONS-I

Coke gasification with carbon dioxide

The industrially produced cokes were subjected to gasification in carbon dioxide atmosphere using two methods, Method I for calculation of activation energy and Method II, i.e. the ASTM standard method for CRI test. The details of the procedures are presented in Chapter 3. The results obtained from the experiments are discussed in this chapter.

4.1. Mass and derivative mass Vs Time plots

The mass and the derivative mass for the four coke samples plotted against time using method I are as shown in Figures 4.1 and 4.2.

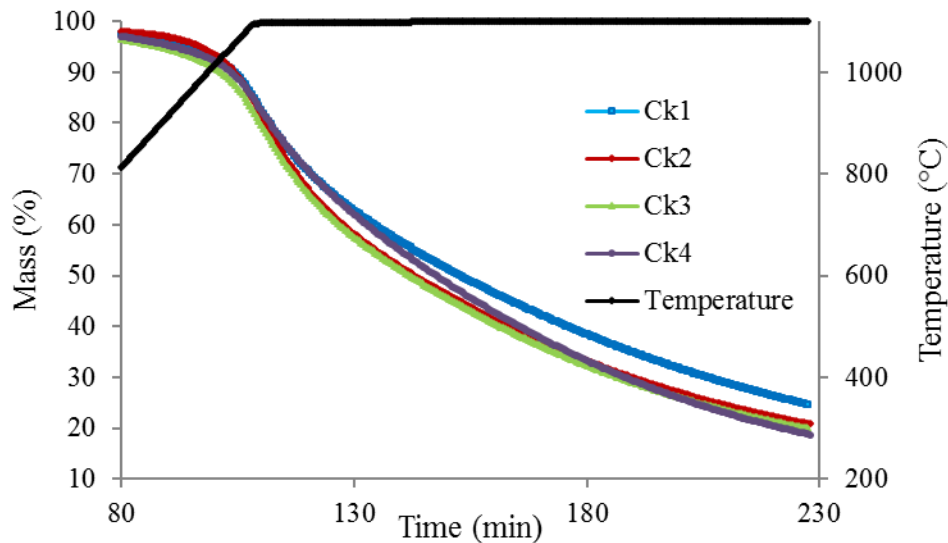


Figure 4.1 Mass Vs time plot (Method I)

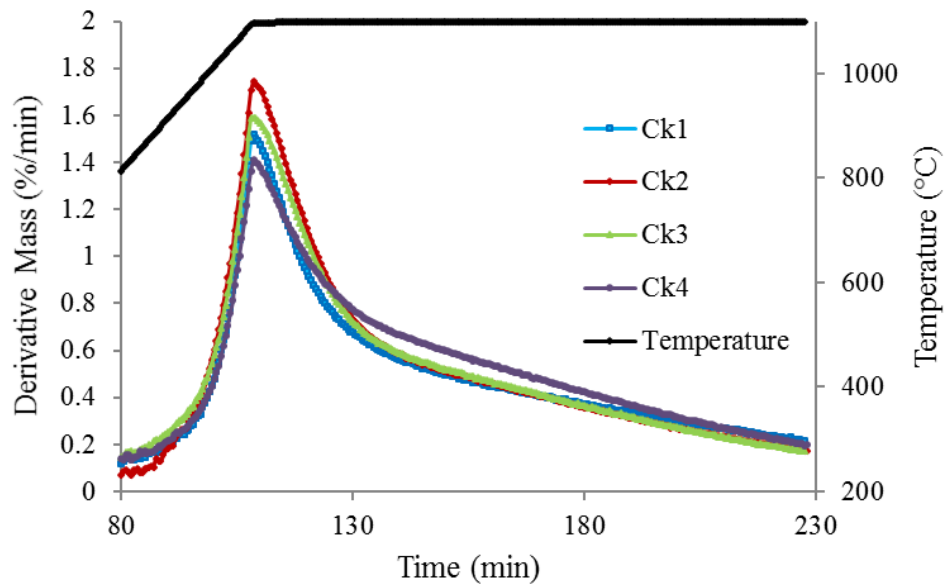


Figure 4.2 Derivative mass vs time plot (Method I)

The mass loss in Ck1 was lower than the other three coke samples. It was also observed that rate of mass loss was higher in Ck2 and Ck3 than the other two cokes, as was reflected by the peaks of the curves.

The mass and the derivative mass for the four coke samples plotted against time using method II are shown in Figures 4.3 and 4.4.

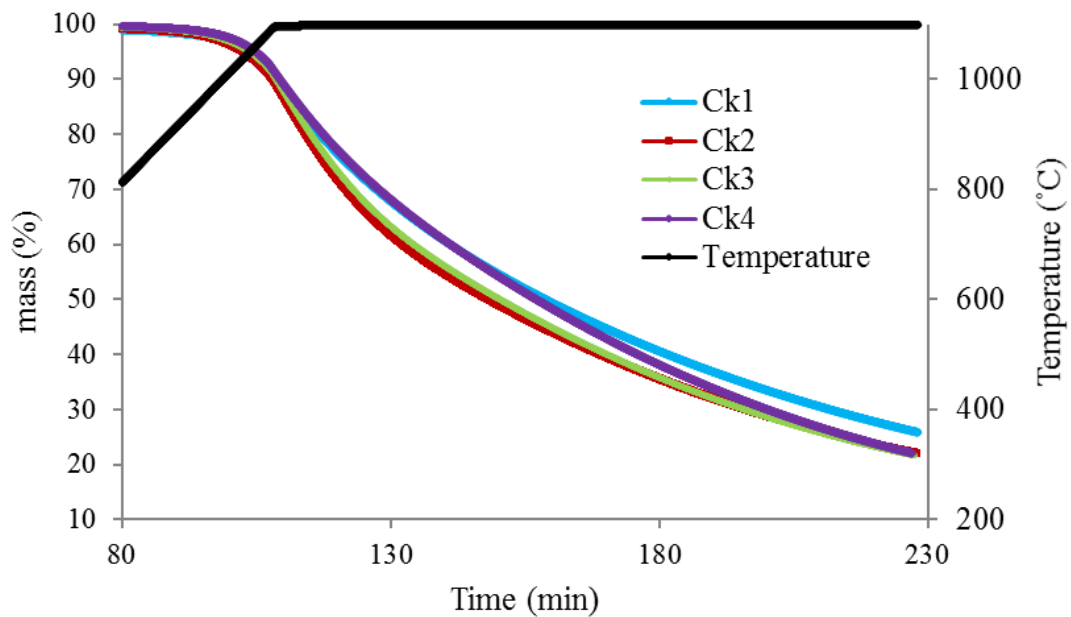


Figure 4.3 Mass loss Vs time plot (Method II)

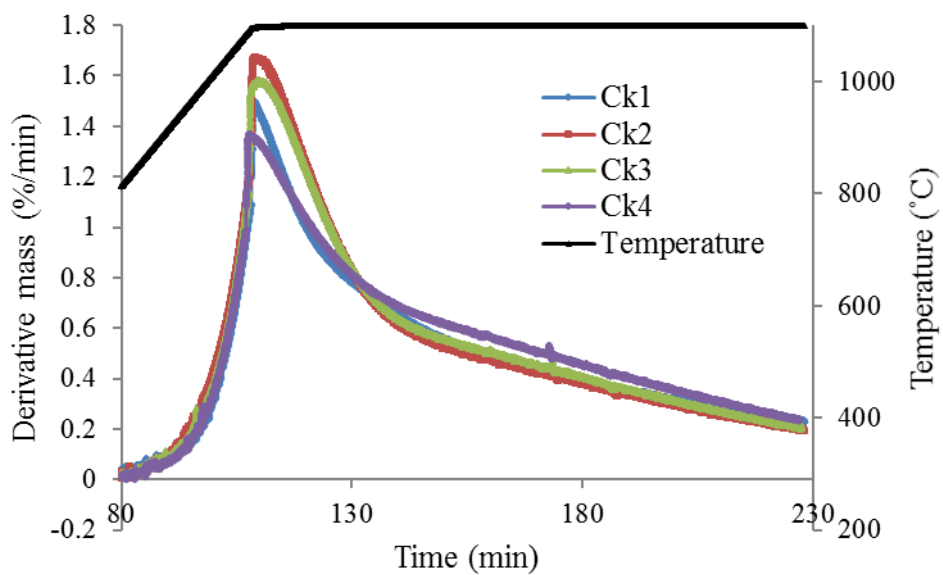


Figure 4.4 Derivative mass loss Vs time plot (Method II)

The mass loss behaviour calculated using Method II showed identical trend for four cokes as that of Method I. The mass loss in Ck1 was lower than the other three coke samples. It was also observed that rate of mass loss was higher in Ck2 and Ck3 than the other two cokes as reflected by the peaks of the curves.

4.2. Activation energy and pre-exponential constant

Kinetic parameters for the CO₂ gasification reaction i.e. the activation energy and pre-exponential constant of the coke samples were calculated using Method I. The detail of the calculating method is discussed in Chapter 3. The Arrhenius for Ck3 is as shown in Figures 4.5. Similar plots were obtained for other samples.

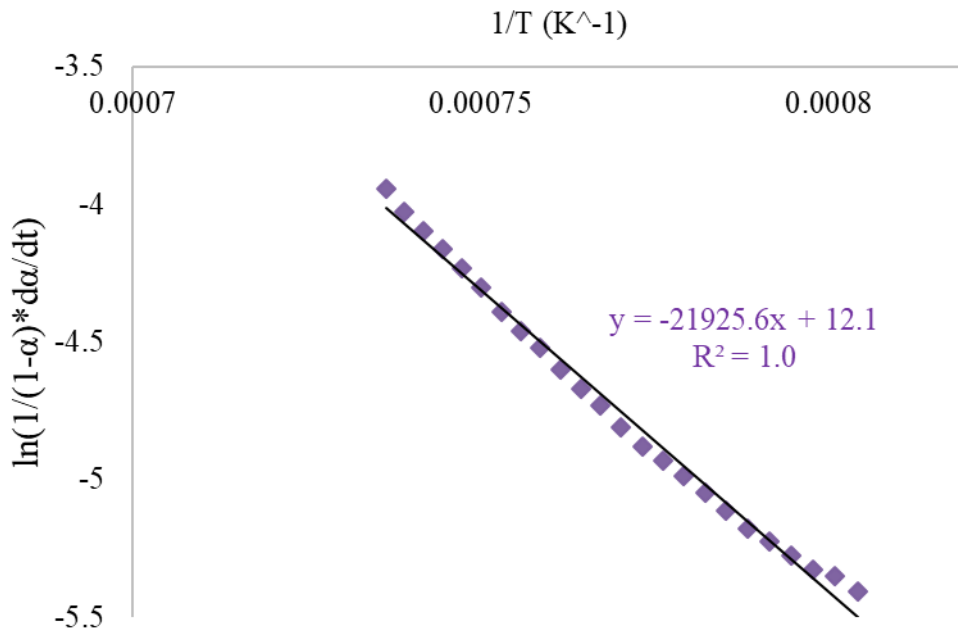


Figure 4.5 Arrhenius plot for Ck3

The activation energy, pre-exponential constant along with correlation coefficients obtained using Direct Arrhenius are as presented in the Table 4.1.

Table 4.1 Activation Energy, Pre-exponential constant, Correlation coefficient of four coke samples using Direct Arrhenius Method

<i>Direct Arrhenius Method</i>				
<i>Sample</i>	Activation Energy, E (kJ/mol)	Standard Deviation (kJ)	Pre-exponential Constant, A	Correlation Coefficient, R²
<i>Ck1</i>	187.5	21.9	5.7E+5	0.99
<i>Ck2</i>	202.5	0.8	1.3E+7	1.00
<i>Ck3</i>	191.6	13.2	5.6E+5	0.99
<i>Ck4</i>	180.8	5.7	9.4E+4	0.99

From the values of activation energy, it is observed that using Direct Arrhenius method, activation energies of the coke samples in 970-1080°C range were similar to literature values (216-266kJ/mol). [Grigore, 2006] [Harris and Smith, 1989]. The particle size, order of reaction, temperature ranges used to calculate activation energy of coke samples are compared with literature data as mentioned in Table 4.2.

Table 4.2 Comparison of literature data and experimental data for Direct Arrhenius

<i>Literature Data</i>					
Temperature Range (°C)	Particle size range (mm)	Energy (kJ/mol)	Order of reaction, n	Reference	Method used
800-920	-1+0.6	216-266	1	[Grigore, 2006]	Direct Arrhenius and ideal gas equation
800-890	-1+0.212	222-266	1	[Grigore, 2009]	Direct Arrhenius
768-917	-0.7+0.2	216-239	0.66	[Harris and Smith, 1991]	Direct Arrhenius & Surface area
<i>Experimental Data</i>					
Temperature Range (°C)	Sample Name	Particle size range (mm)	Activation energy (kJ/mol)	Order of reaction, n	Method used
970-1080	Ck 1	-0.25	187.5	1	Direct Arrhenius
	Ck 2		202.5		
	Ck 3		199.6		
	Ck 4		180.7		

4.3. Conversion factor during soaking period and CRI

The conversion factors during soaking period at 1100°C were calculated as discussed in Chapter 3. The conversion factors along with CRI values of the samples are as mentioned in Table 4.3 and the CRI values of the four cokes were plotted against conversion factor as shown in Figure 4.6.

It was observed that for method I, conversion of the samples at 1100°C showed linear relation with Coke Reactivity Index of the cokes. However, for method II, Ck3 and Ck4 had same conversion and as a result, no linear trend was observed with the CRI of the cokes.

Table 4.3 Conversion during soaking period at 1100°C and CRI of the cokes

<i>Sample</i>	<i>Conversion factor, α (Method I)</i>	<i>Conversion factor, α (Method II)</i>	<i>Coke Reactivity Index, CRI</i>
<i>Ck1</i>	0.79	0.79	21.6
<i>Ck2</i>	0.78	0.85	22.1
<i>Ck3</i>	0.83	0.86	24.4
<i>Ck4</i>	0.87	0.86	26.2

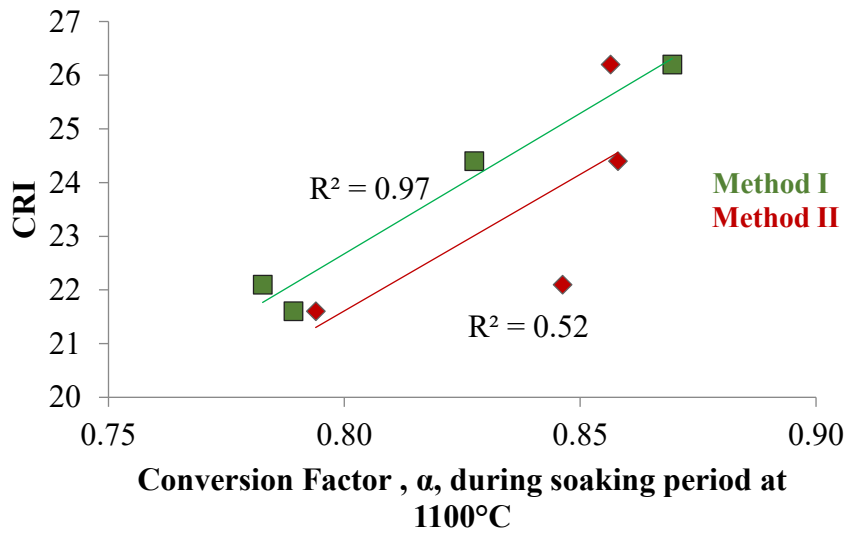


Figure 4.6 CRI plotted against conversion factor at soaking period

4.4 Conclusions

The following conclusions were drawn from the results in this chapter.

- For calculation of activation energy, Direct Arrhenius method is reliable since the values match closely with those in literature.

- The conversion of coke in carbon dioxide atmosphere at 1100°C in thermogravimetric analysis is found to have a significant linear relation with CRI of the cokes. Hence, TGA can be used as an alternative to predict CRI of cokes provided that a large variety of coke samples are used.

5. RESULTS AND DISCUSSIONS- II

Characterization of cokes prepared in horizontal tube furnace

Coal carbonization was carried out in a horizontal tube furnace as discussed in detail in Chapter 3. Several characterization techniques were carried out on the products as discussed below.

5.1. Effect of heating rate during de-volatilization on coking

The four coal samples were carbonized using two different heating rates during the de-volatilization period. The results are as discussed below.

5.1.1. Coking yield

The yield (%) of the carbonization products are as mentioned in the Table 5.1.

Table 5.1 Effect of heating rate on coking yield

<i>Heating Rate* (°C/min)</i>	<i>MCX</i>	<i>MCN</i>	<i>EC</i>	<i>DC</i>
5	76.23	78.47	78.90	79.80
2.5	76.94	76.77	77.64	80.37

*Heating Rate during de-volatilization (300 to 500°C)

It is noticeable that there was little effect of heating rate of de-volatilization on the yield of coke. This is because when the heating rate are sufficiently low (5 °C/min), further decrease in heating rate does not effect on yield of coke [Warren, 1938]. The yield for all the cokes was similar to values in literature for final soaking temperature of 900 °C [Kobayashi, 1977].

5.1.2. Ash analysis

Coke samples were subjected to ash analysis using ASTM D3174 method as discussed in details in Chapter 3. The ash percentage in the cokes produced using 5 °C/min and 2.5 °C/min heating rate during de-volatilization period are as mentioned in Table 5.2.

Table 5.2 Effect of heating rate on ash content of cokes

<i>Heating rate* (°C/min)</i>	<i>MCX</i>	<i>EC</i>	<i>DC</i>	<i>MCN</i>
5	11.80	14.29	20.27	8.99
2.5	11.98	15.21	19.99	12.13

Heating rate during de-volatilization (300 to 500°C)

It was observed that ash content of the most of the cokes had very little change with decrease in heating rate during de-volatilization period. For DC, ash content was already high for metallurgical coke as the normal range is close to 10% [Dombrovskii, 1988]. Hence, for DC, both heating rate gave rise to similarly high ash content.

5.1.3. CO₂ gasification

The coke samples were subjected to gasification in carbon dioxide using ASTM 5341 method, as discussed in details in chapter 3. The total mass loss during the experiments and the conversion in CO₂ during the soaking period at 1100°C are as mentioned in Table 5.3 and shown in Figure 5.1.

Table 5.3 Effect of heating rate on conversion in CO₂ at 1100 °C

<i>Heating rate (°C/min)</i>	<i>MCX</i>	<i>EC</i>	<i>DC</i>	<i>MCN</i>
5	0.74	0.79	0.73	0.75
2.5	0.75	0.89	0.84	0.75

**Heating Rate during de-volatilization (300-500°C)*

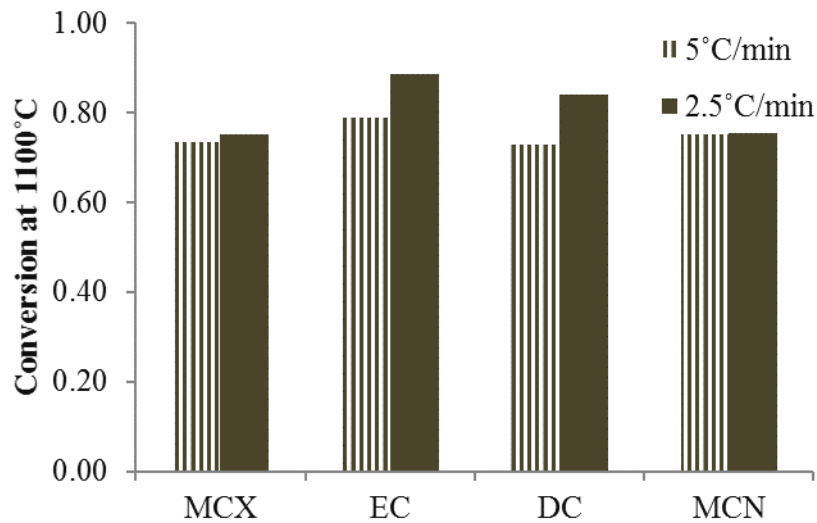


Figure 5.1 Effect of heating rate on conversion in CO₂ at 1100 °C

It could be observed that reducing heating rate during de-volatilization period increased the conversion at CO₂ atmosphere at 1100 °C in two of the samples, EC and DC. This can be explained based on the change in porosity with heating rate. Lowering the heating rate had increased porosity of EC and DC. Increase in porosity had resulted in increased reactivity with CO₂, i.e. conversion

had increased [Peter, 1962]. For the MCX and MCN samples, conversion was not effected significantly with change in heating rate during de-volatilization period.

5.1.4. Image analysis of coke

Image analysis was carried out and porosity (%) was calculated as mentioned in details in Chapter 3. The microscopic images of MCX produced using 5 °C /min and 2.5 °C/min heating rate are as mentioned in Figure 4.10. Similar images were obtained for the other samples.

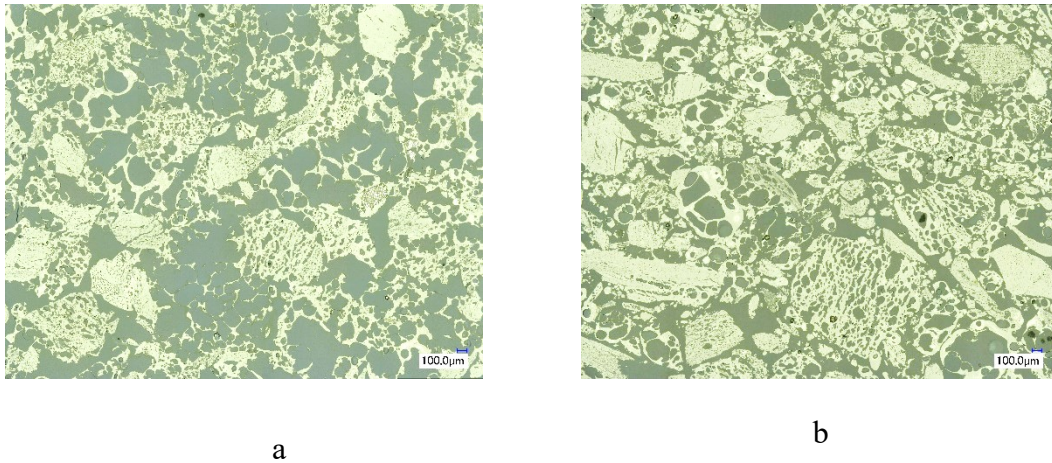


Figure 5.2 Stitched image of MCX at a) 5 °C /min and b) 2.5 °C /min (250X)

Total porosity (%) of the samples were as mentioned below in Table 5.4 and in Figure 5.3.

It can be observed that for two of the samples, EC and DC, lowering the heating rate during de-volatilization slightly increased the total porosity of the coke samples and in case of the other two, there was decrease in porosity. Porosity in all of the coke samples were found to be within data reported in the literature [Xing. , 2013] [Loison , 1989].

Table 5.4 Effect of heating rate during de-volatilization on total porosity (%)

<i>Heating rate* (°C/min)</i>	<i>Sample</i>	<i>Average Porosity (%)</i>	<i>Standard deviation</i>
2.5	MCX	54.11	1.09
	EC	56.11	0.86
	DC	63.92	1.01
	MCN	54.19	0.21
5	MCX	57.98	0.39
	EC	54.29	1.04
	DC	63.21	0.60
	MCN	60.89	0.37

*Heating rate during De-volatilization (300 to 500°C)

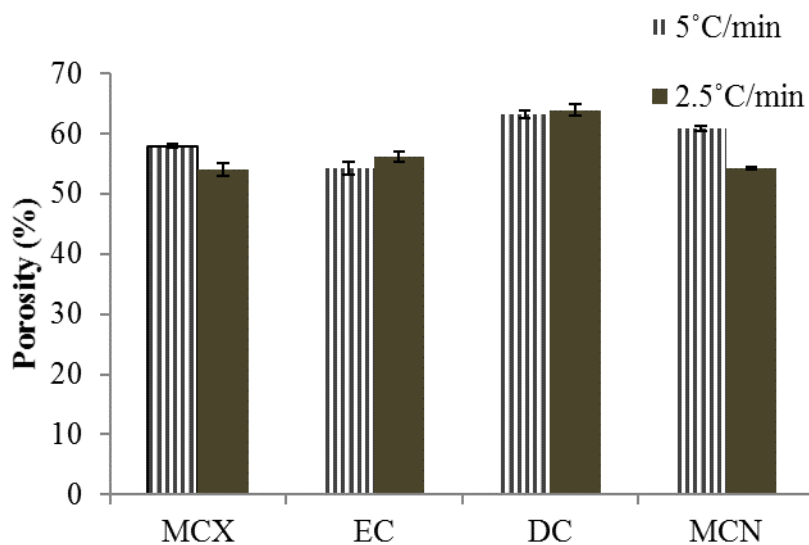


Figure 5.3 Effect of heating rate during de-volatilization on total porosity (%)

5.1.5. Extent of graphitization

Raman spectroscopy was carried out on the coke samples as discussed in details in Chapter 3. Two distinct peaks were obtained in the spectrum obtained at around 1300cm^{-1} and 1600cm^{-1} as was expected [Mennella, 1995]. Plot of DC spectrum is as mentioned in the Figure below.

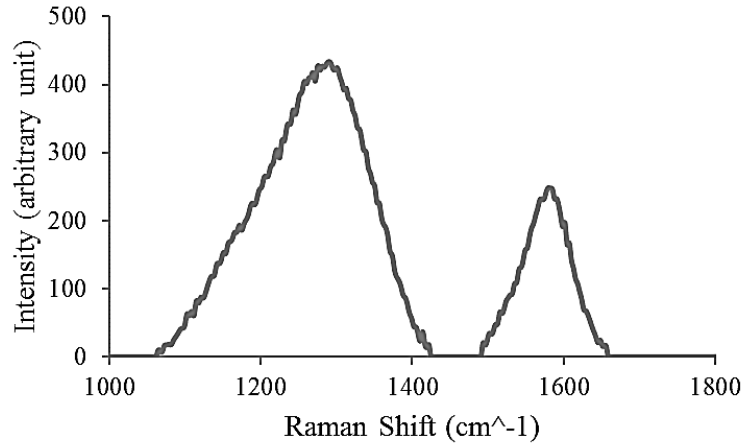


Figure 5.4 Raman Spectrum of DC

Similar plots were obtained for all other samples. The extent of graphitization was calculated using the ratio of the area under the two curves. The area under each curve, A_d , A_g and the extent of graphitization, i.e., ratio $\frac{A_g}{A_g+A_d}$ are as mentioned in Table 5.5 and the extent of graphitization for all the samples are compared in Figure 5.5.

Table 5.5 Effect of heating rate during de-volatilization period on extent of graphitization of cokes

<i>Sample</i>	<i>Heating rate</i> (°C/min)	<i>Area, A_d</i>	<i>Area, A_g</i>	<i>Extent of graphitization,</i> $\frac{A_g}{A_g + A_d}$	<i>Standard Deviation</i>
<i>MCX</i>	5	31944	10643	0.25	0.004
	2.5	46054	19104	0.29	0.003
<i>EC</i>	5	34683	10837	0.24	0.000
	2.5	57668	21443	0.27	0.018
<i>DC</i>	5	84148	24645	0.23	0.003
	2.5	58591	18159	0.24	0.007
<i>MCN</i>	5	46761	15765	0.25	0.001
	2.5	60698	23919	0.28	0.008

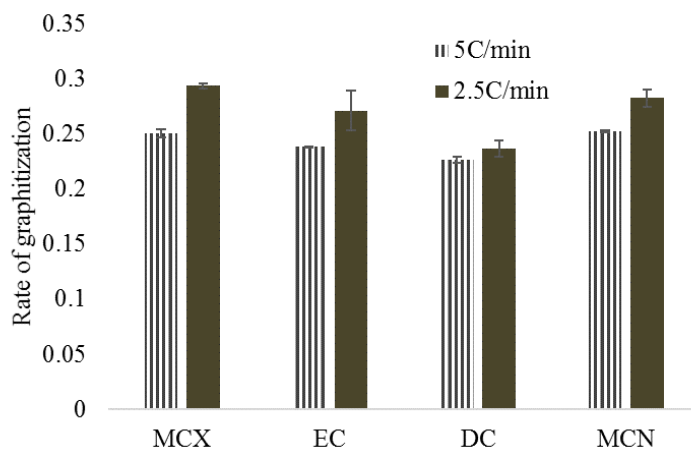


Figure 5.5 Effect of heating rate during de-volatilization period on extent of graphitization

It was observed that decreasing the heating rate during de-volatilization period increased the extent of graphitization of the coke samples. As more time was allowed during the heating period, it enhanced the degree of coking.

5.2. Effect of addition of binders

5.2.1. Effect of addition of asphaltene

Samples were prepared using asphaltene as binder as discussed in details in Chapter 3. The different characterization techniques carried out on the samples are as discussed below.

5.2.1.1. Ash Analysis

All the coke samples were subjected to ash analysis using ASTM D3174 method as discussed in details in Chapter 3. The ash percentages in the cokes produced using different amount of asphaltene are as mentioned in Table 5.6 and shown in Figure 5.6.

Table 5.6 Effect of asphaltene on ash content of cokes

<i>Ash (%)</i>	<i>GC</i>	<i>DC</i>
<i>pure</i>	8.08	19.92
<i>10Asp</i>	8.80	20.73
<i>20Asp</i>	7.75	17.7
<i>10AFC10Asp</i>	7.63	16.35

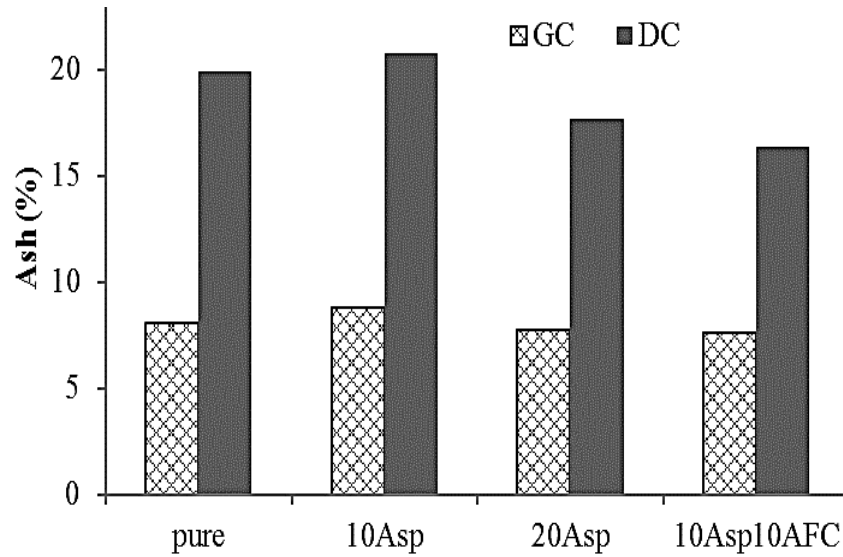


Figure 5.6 Effect of asphaltene on ash content of cokes

Addition of 10% asphaltene caused a slight increase in ash content in both cokes. It was also observed that addition of 10% ash free coal along with 10% asphaltene and addition of 20% asphaltene reduced ash content of the cokes.

5.2.1.2. CO₂ gasification

The coke samples were subjected to gasification in Carbon dioxide as discussed in details in chapter 3. The total mass loss during the experiments and the conversion in CO₂ during the soaking period at 1100°C are as mentioned in Table 5.7.

Table 5.7 Effect of asphaltene addition on conversion during the isothermal period in CO₂ and total mass loss

<i>Sample</i>	<i>Conversion at 1100°C</i>	<i>Total mass loss (%)</i>
<i>DCR</i>	0.86	69.15
<i>DC10Asp</i>	0.86	69.61
<i>DC20Asp</i>	0.87	72.33
<i>DC10AFC10Asp</i>	0.84	71.38
<i>GCR</i>	0.98	92.81
<i>GC10Asp</i>	0.99	92.177
<i>GC20Asp</i>	1.00	93.815
<i>GC10AFC10Asp</i>	0.98	93.569

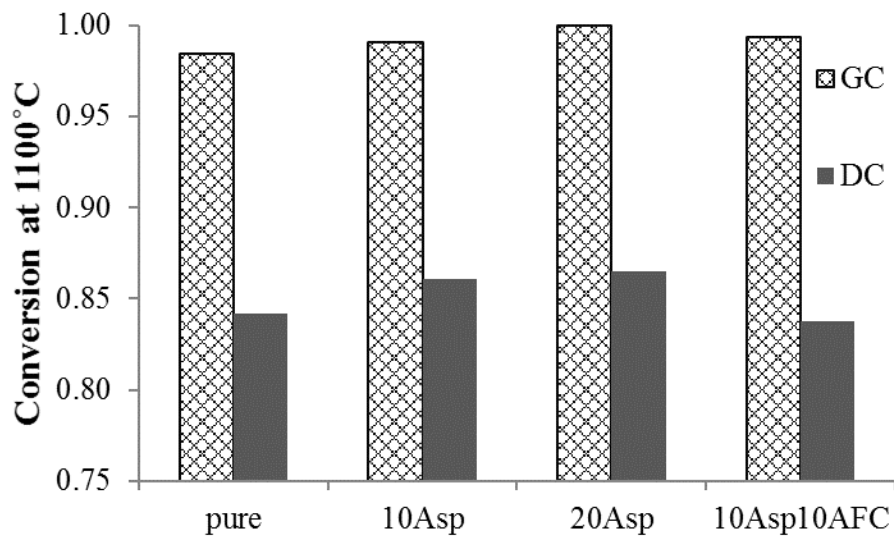
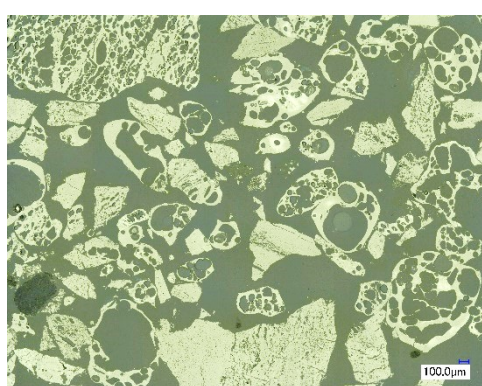


Figure 5.7 Effect of asphaltene addition on conversion during isothermal period

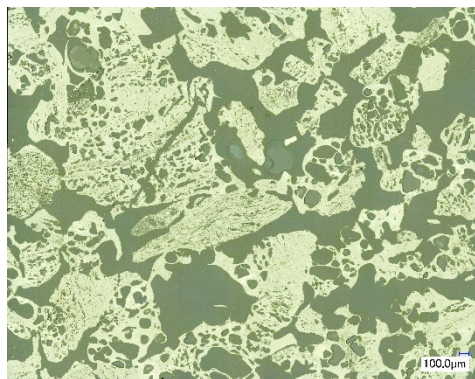
From Figure 5.7, it could be observed that asphaltene addition had little effect on product of the sub-bituminous coal, GC , which was of lower rank than DC and most of the mass had been consumed within 2 hrs in CO₂ environment , as suggested by literature [Ye, 1998]. The conversion for the product of the coking coal, DC, had slightly increased with asphaltene addition. However for the sample with 10% asphaltene and 10% ash free coal, conversion had decreased which suggests that asphaltene addition had little effect on reactivity but ash free coal might have an effect.

5.2.1.3. Image analysis of coke

Image analysis was carried out and porosity (%) was calculated as mentioned in detail in Chapter 3. The microscopic images of DC with different amounts of asphaltene are as mentioned in Figure 4.16. Similar images were obtained for the samples of GC. Total porosity (%) of the samples was as mentioned below in Table 5.8 and in Figure 5.8.



a



b

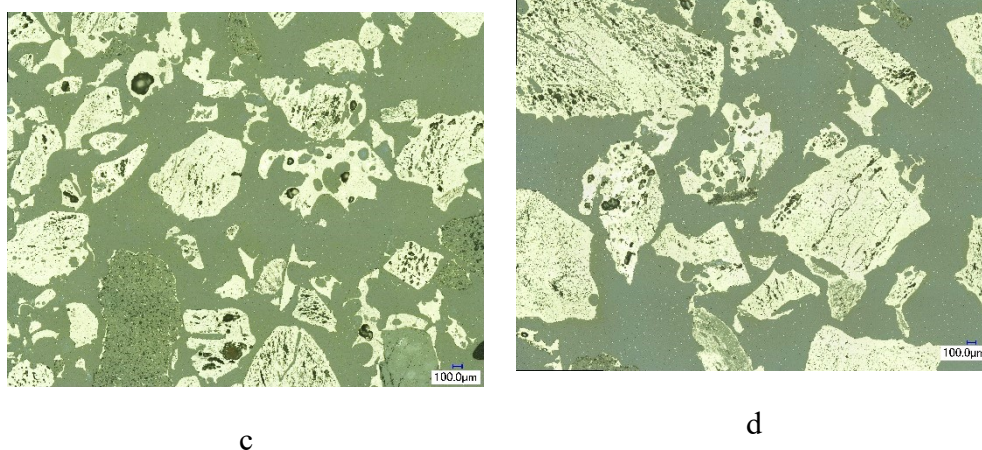


Figure 5.8 Stitched image of a) pure DC b) DC10Asp c) DC20Asp d) DC10AFC10Asp (250X)

Table 5.8 Effect of asphaltene addition on total porosity (%) of coke samples

<i>Sample</i>		<i>Average porosity (%)</i>	<i>Standard Deviation</i>
<i>DC</i>	pure	62.90	0.2
	10Asp	54.91	0.1
	20Asp	69.22	0.63
	10AFC10Asp	61.71	0.66
<i>GC</i>	pure	58.07	1.387
	10Asp	47.71	0.09
	20Asp	80.83	2.07
	10AFC10Asp	71.88	0.61

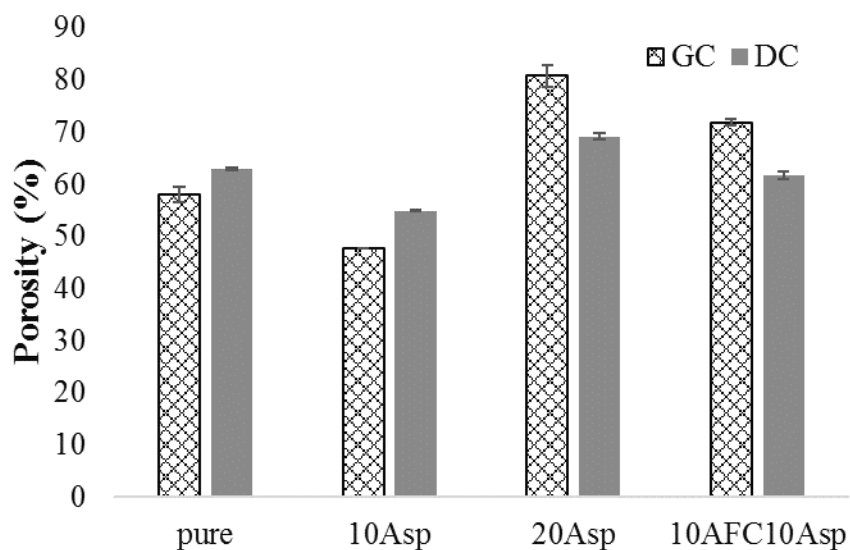


Figure 5.9 Effect of asphaltene addition on total porosity (%)

The total porosity values for the samples with up to 10% asphaltene addition were similar to the range observed in industrial cokes [Xing, 2013] [Loison, 1989]. It was observed that total porosity of both DC and GC decreased with addition of 10% asphaltene and it acted as a good binder. Upon addition of asphaltene beyond 10%, the porosity increased for both DC and GC. It could also be observed that when 10% asphaltene was added along with 10% ash free coal, porosity increase for both DC and GC was lower than that with 20% asphaltene but greater than that with 10% asphaltene. This reflects that the combined contribution of asphaltene and ash free coal has no better effect on porosity than addition of 10% of individual binder.

5.2.1.4. Extent of graphitization

Raman spectroscopy showed two distinct peaks in the spectrum obtained at around 1300cm^{-1} and 1600cm^{-1} as was expected [Mennella, 1995]. Plot of DCR spectrum is as mentioned in the Figure below. Similar plots were obtained for all other samples.

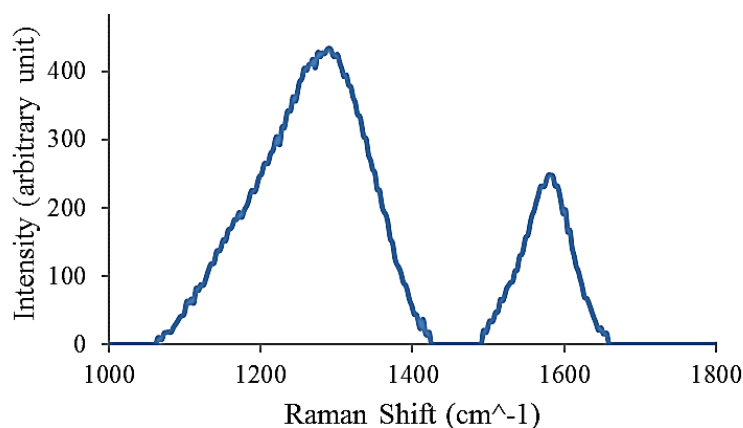


Figure 5.10 Raman Spectrum of DCR

The extent of graphitization was calculated using the ratio of the area under two curves. The area under each curve, A_d , A_g and the extent of graphitization, i.e., ratio $\frac{A_g}{A_g + A_d}$ are as mentioned in Table 5.9 and the extent of graphitization for all the samples are compared in Figure 5.11.

Table 5.9 Area under Ad, Ag and extent of graphitization for the samples

	<i>Sample</i>	<i>Area,</i> <i>A_d</i>	<i>Area,</i> <i>A_g</i>	<i>Extent of graphitization,</i>	<i>Standard</i> <i>Deviation.</i>
				$\frac{A_g}{A_g + A_d}$	
DC	Pure	67264	19192	0.224	0.020
	10Asp	40378	17074	0.29	0.002
	20Asp	75055	22578	0.23	0.002
	10AFC10Asp	37377	11611	0.24	0.003
GC	Pure	79487	22594	0.22	0.005
	10Asp	95663	27541	0.22	0.005
	20Asp	113869	30898	0.21	0.014
	10AFC10Asp	72222	20067	0.22	0.009

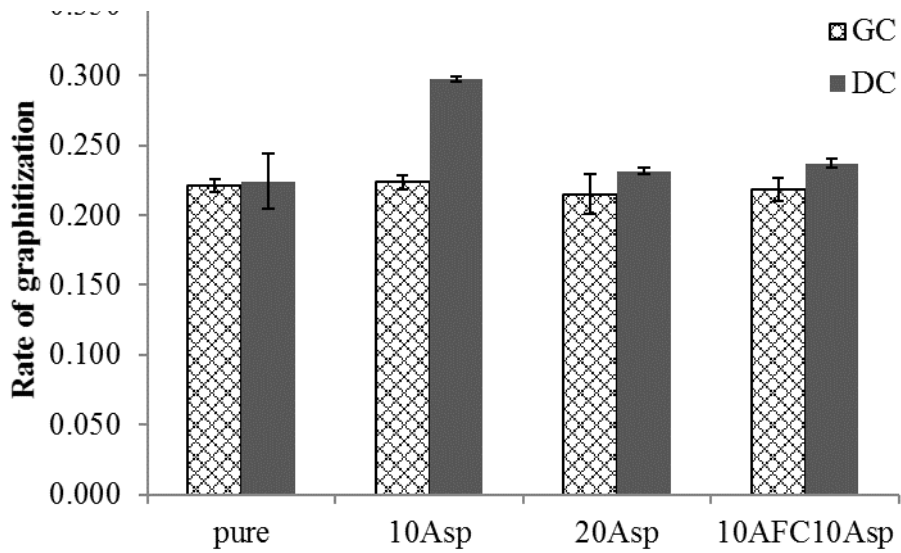


Figure 5.11 Effect of asphaltene addition on extent of graphitization

Addition of asphaltene on coking coal (DC) slightly increased the extent of graphitization in the respective coke for 10% addition. This had occurred as asphaltene can yield up to 47% of coke

[Trejo, 2010]. However, for higher amount of asphaltene, the effect on graphitization was lower. The effect of extent of graphitization on sub-bituminous coal was negligible on the respective coke.

5.2.2. Effect of ash free coal addition

The different characterization techniques were carried out on the samples as discussed below.

5.2.2.1. Ash analysis

The ash percentage in the cokes produced using different amount of ash free coal was as mentioned in Table 5.10 and shown in Figure 5.12.

Table 5.10 Effect of ash free coal on ash content of cokes

<i>Ash (%)</i>	<i>GC</i>	<i>DC</i>
<i>pure</i>	8.08	19.92
<i>10AFC</i>	9.89	15.00
<i>20AFC</i>	7.73	17.55
<i>10AFC10Asp</i>	7.63	16.35

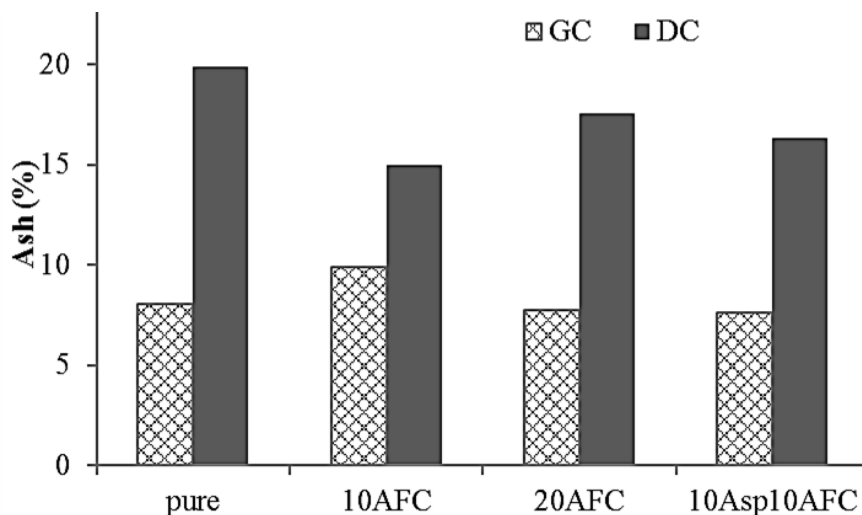


Figure 5.12 Effect of ash free coal on ash content of cokes

For the coking coal, DC, addition of ash free coal reduced the total ash content of the coke samples, as ash free coal has minimal amount of ash content [M. Rahman, 2012]. For the sub-bituminous coal, GC, addition up to 10% ash free coal increased the ash content of the respective coke slightly; since the coke GC, already had low ash content, there was little affect with addition of only 10% AFC. Further addition of AFC, however, decreased the ash content.

5.2.2.2. CO₂ gasification

The total mass loss during the experiments and the conversion in CO₂ during the soaking period at 1100°C are as presented in Table 5.11 and compared in Figure 5.13.

Table 5.11 Effect of ash free coal addition on conversion during isothermal period in CO₂ and total mass loss

<i>Sample</i>	<i>Conversion at 1100°C</i>	<i>Total mass loss (%)</i>
<i>DCR</i>	0.86	69.15
<i>DC10AFC</i>	0.94	75.51
<i>DC20AFC</i>	0.77	64.58
<i>DC10AFC10Asp</i>	0.84	71.38
<i>GCR</i>	0.98	92.81
<i>GC10AFC</i>	1.00	91.76
<i>GC20AFC</i>	1.00	94.42
<i>GC10AFC10Asp</i>	0.98	93.57

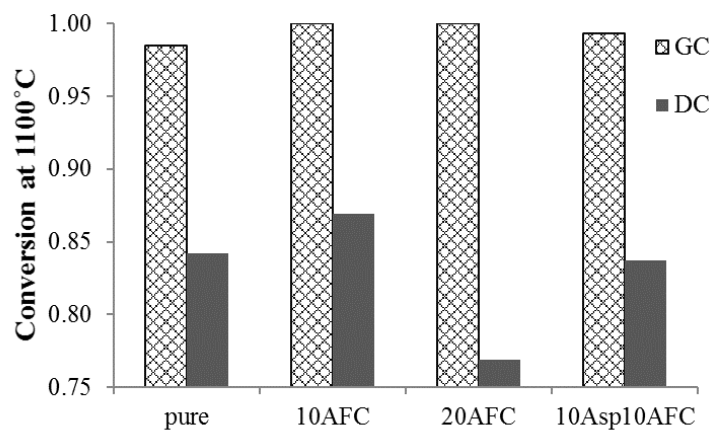


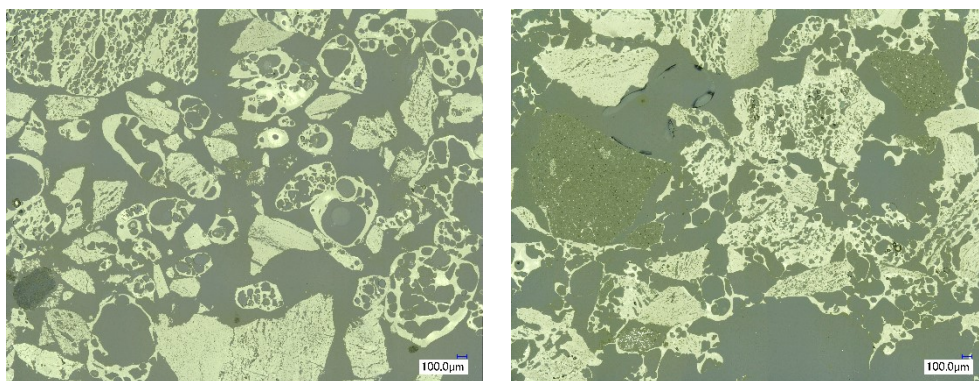
Figure 5.13 Effect of ash free coal addition on conversion during isothermal period

It was observed that ash free coal addition had little effect on product of the sub-bituminous coal and most of the mass had been consumed within 2 hrs in CO₂ environment. The conversion for the product of the coking coal, DC, had slightly increased with addition of 10% ash free coal. This is

because AFC has minimal ash content and more of convertible mass. However for higher amount of ash free coal, i.e., the sample with 20% ash free coal and also the one with 10% asphaltene and 10% ash free coal, conversion decreased which suggests that ash free coal addition has some potential to reduce reactivity of coke.

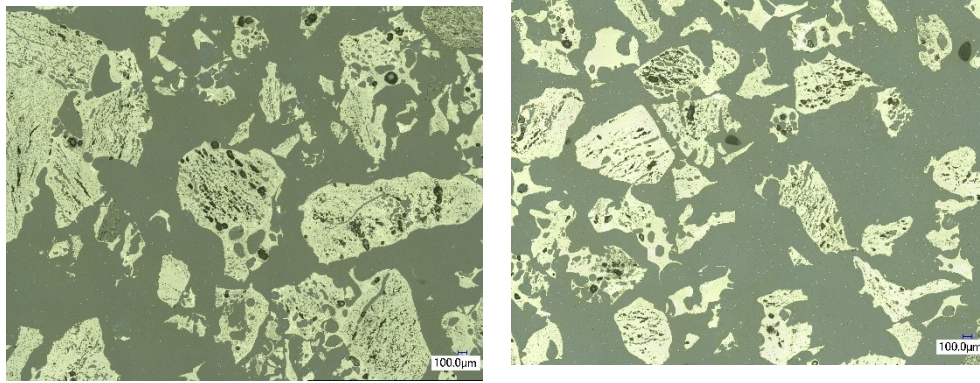
5.2.2.3. Image analysis of coke

All the samples were subjected to image analysis and porosity (%) was calculated. The microscopic images of DC with different amounts of ash free coal are mentioned in Figure 5.14. Similar images were obtained for the samples with GC. Total porosity (%) of the samples was as mentioned below in Table 5.12 and in Figure 5.15.



a

b



c

d

Figure 5.14 Stitched image of a) pure DC b) DC10AFC c) DC20AFC d) DC10AFC10Asp
(250X)

Table 5.12 Effect of ash free coal addition on total porosity (%) of cokes

<i>Sample</i>		<i>Average porosity (%)</i>	<i>Standard Deviation</i>
DC	pure	62.9	0.1
	10AFC	58.1	0.2
	20AFC	62.9	1.16
	10AFC10Asp	61.7	0.66
GC	pure	58.0	1.38
	10AFC	49.9	0.10
	20AFC	61.9	1.79
	10AFC10Asp	71.8	0.61

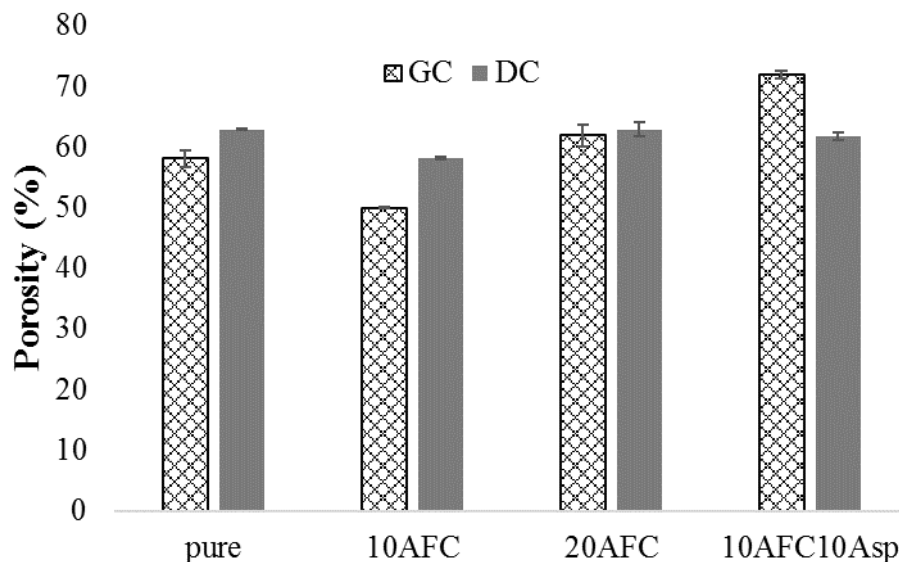


Figure 5.15 Effect of ash free coal addition on total porosity (%)

The total porosity values for most of the samples, except GC10AFC10Asp, were similar to the range observed for industrial cokes [Xing, 2013] [Loison, 1989]. It could be observed that total porosity of both DC and GC decreased with addition of 10% ash free coal. This accounts for the minimal mineral content in AFC [Rahman, 2013] and more organic mass content. Addition of ash free coal beyond 10% had no significant effect on DC but for GC, the porosity increased slightly. It was also observed that porosity increased for both DC and GC when 10% asphaltene was added along with 10% ash free coal, which reflects the contribution of asphaltene on porosity.

5.2.2.4. Extent of graphitization

Two distinct peaks were obtained in the Raman spectrum at around 1300cm^{-1} (peak of disoriented carbon, d) and 1600cm^{-1} (peak of graphitic carbon, g) similar to literature [Mennella, 1995]. The

curve for DCR sample is as shown in the Figure 5.16. Similar plots with two peaks were obtained for all other samples.

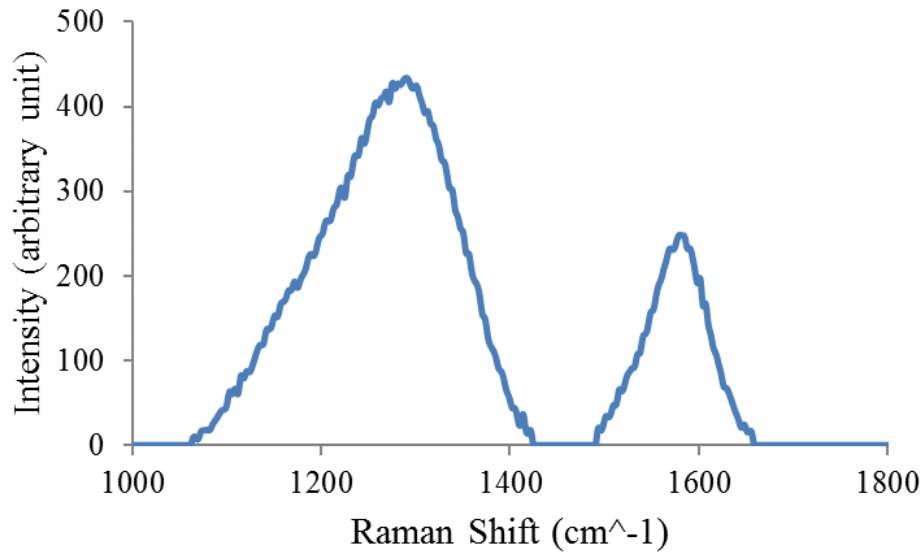


Figure 5.16 Raman Spectrum of DCR

The area under each curve, A_d , A_g and the extent of graphitization, i.e., ratio $\frac{A_g}{A_g + A_d}$ are as mentioned in Table 5.13. Also, the extent of graphitization for all the samples is compared in Figure 5.17.

It was observed that addition of ash free coal on coking coal, DC, had slightly increased the extent of graphitization in the respective cokes. It could also be observed that sub-bituminous coal, GC, had little effect on rate of the graphitization of the respective coke and with more than 10% ash free coal, the extent of graphitization slightly decreased.

Table 5.13 Effect of ash free coal addition on Ad, Ag and extent of graphitization for the samples

	<i>Sample</i>	<i>Area, A_d</i>	<i>Area, A_g</i>	<i>Extent of graphitization, $\frac{A_g}{A_g + A_d}$</i>	<i>Standard Deviation</i>
DC	pure	67264	19191	0.22	0.020
	10AFC	57004	19508	0.26	0.001
	20AFC	40571	13751	0.25	0.002
	10AFC10Asp	37377	11611	0.24	0.003
GC	pure	79487	22594	0.22	0.005
	10AFC	74148	22043	0.23	0.003
	20AFC	89160	24590	0.22	0.007
	10AFC10Asp	82225	21556	0.22	0.009

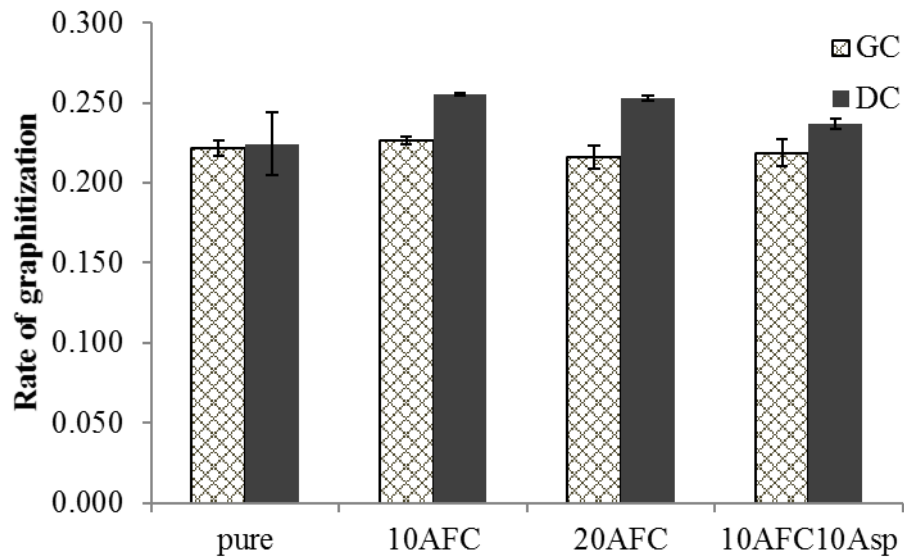


Figure 5.17 Effect of ash free coal addition on Extent of graphitization

5.3. Conclusions

The following conclusions can be drawn from the results of this study.

- *Effect of heating rate:* When carbonizing coal in lab scale, the heating rate during devolatilization has negligible effect on percentage yield of cokes. However, the conversion in CO₂, porosity and extent of graphitization i.e. the degree of coking increases upon lowering the heating rate.
- *Addition of asphaltene:* It causes higher reactivity in the coke produced from bituminous coal. However, the total porosity decreases and the extent of graphitization increases, resulting in slightly improved coke. Addition of asphaltene in sub-bituminous coal shows no improvement in reactivity of the produced coke and the mass was completely consumed during soaking period at CO₂ atmosphere. Moreover, there is no significant change in degree of coking but porosity increases. Hence, sub-bituminous coal with addition of asphaltene as binder is not suitable for use in blast furnace.
- *Addition of ash free coal:* In bituminous, coking coal, it causes decrease in coke reactivity and porosity also decreases when more than 10% ash free coal is used as binder. Moreover, extent of graphitization also increases slightly. Hence, ash free coal can be used as binder for improving the quality of a bituminous coal. Addition of ash free coal in sub-bituminous coal had no positive effect on reactivity of the cokes as the mass was completely consumed in CO₂. However, for up to 10% ash free coal in sub-bituminous coal, extent of graphitization slightly increases and porosity decreases

slightly. Overall, the sub-bituminous coal with ash free coal as binder is not suitable as a replacement of metallurgical coke in blast furnace.

- This study has been carried out on a preliminary basis to see the effect of asphaltene and ash free coal addition on respective coke properties. Further study is required in this area for getting conclusive remarks on these two additives.

6. CONCLUSIONS AND FUTURE WORK

6.1. Conclusions

The following conclusions can be drawn from the research carried out in this thesis.

- For calculation of kinetic parameters using non-isothermal conditions, use of Arrhenius equation is reasonable and the values obtained are comparable to the literature range.
- Conversion of coke in carbon dioxide during isothermal soaking period in Thermo-Gravimetric Analysis (TGA) was correlated with Coke Reactivity Index (CRI) and there was a linear relation between the two. Hence, conversion in TGA can be used widely to study reactivity of different cokes.
- When coal is carbonized in a lab-scale, heating rate during de-volatilization period has little effect on yield percentage of coke. Meanwhile, ash content, conversion in CO₂ and extent of graphitization, i.e., degree of coking, of the coke increases when a lower heating rate is used.
- When asphaltene was used as a binder in bituminous coking coal during carbonization in a lab-scale, ash content of respective cokes decreased when asphaltene was added beyond 10%. The conversion of coke obtained from coking coal has negative effect on addition of asphaltene, i.e., upon addition of asphaltene, reactivity in carbon dioxide increased. Asphaltene addition, however, causes some improvement in coke. For asphaltene addition up to 10%, extent of graphitization increased and total porosity of the cokes decreased.
- Upon addition of asphaltene in sub-bituminous coal, the product completely gets consumed in carbon dioxide which implies that asphaltene causes no significant improvement in CO₂ reactivity of cokes from sub-bituminous coal. Moreover, asphaltene addition has no significant change in

extent of graphitization and porosity increases. Hence, use of asphaltene as a binding agent in sub-bituminous coal is not suitable for coal carbonization

- When ash free coal was used as binder with bituminous coal, for more than 10% addition, ash content of coke decreases, so does the reactivity in CO₂ and the porosity. In addition, the extent of graphitization increases slightly. Hence, addition of ash free coal has the potential to be used widely as a binder in coking coal to improve its quality.
- Upon addition of ash free coal in sub-bituminous coal, neither there was noticeable effect on ash content of the coke nor any improvement in the coke reactivity with CO₂. However, extent of graphitization increases slightly and the total porosity decreased for addition up to 10% ash free coal. In brief, product of sub-bituminous coal has little significance to be used as an alternative for metallurgical coke.

6.2. Future Work

The following future works areas are recommended.

- For calculation of kinetic parameters for CO₂ gasification of cokes, more non-isothermal methods can be used and isothermal methods can be tried.
- A model can be developed to predict CRI of coke using conversion in TGA, provided that a large variety of cokes are used in the work.
- Study of role of specific coal minerals on coke properties can be carried out by addition of minerals such as quartz, alumina and other chemical components in the coal .
- Since there is a limited resource of coking coal in the world, it is recommended to blend small amount of sub-bituminous coals with coking coals and to study the properties in order to estimate the optimal coal-blending ratio.

BIBLIOGRAPHY

Álvarez, R., Díez, M. A., Barriocanal, C., Díaz-Faes, E., & Cimadevilla, J. L. G. (2007). An approach to blast furnace coke quality prediction. *Fuel*, 86(14 SPEC. ISS.), 2159–2166. <http://doi.org/10.1016/j.fuel.2006.11.026>

ASTM. (1999). D5341 Standard Test Method for Measuring Coke Reactivity Index (CRI) and Coke Strength After Reaction (CSR), 99(Reapproved), 3–7.

ASTM. (2015). Standard Terminology of. *ASTM*, 1–14.

Belden, A. W. (1913). The Beehive Coke Oven Industry of the United States. *Journal of Industrial & Engineering Chemistry*, 5(1), 71–73.

Benk, A. (2010). Utilisation of the binders prepared from coal tar pitch and phenolic resins for the production metallurgical quality briquettes from coke breeze and the study of their high temperature carbonization behaviour. *Fuel Processing Technology*, 91(9), 1152–1161.

Benk, A., Talu, M., & Coban, A. (2008). Phenolic resin binder for the production of metallurgical quality briquettes from coke breeze: Part I. *Fuel Processing Technology*, 89(1), 28–37.

Bermúdez, J. M., Arenillas, A., Luque, R., & Menéndez, J. A. (2013). An overview of novel technologies to valorise coke oven gas surplus. *Fuel Processing Technology*, 110, 150–159.

Burger, John R. Coke reclaiming pays off. (1979) *Coal age*, 84 (11), pp. 114-120

Chun, Y., Kim, S. J., Millar, G. J., Mulcahy, D., Kim, I. S., & Zou, L. (2017). Forward osmosis as a pre-treatment for treating coal seam gas associated water: Flux and fouling behaviour. *Desalination*, 403, 144-152.

Coats, A. W., & Redfern, J. P. (1964). Kinetic parameters from thermogravimetric data. *Nature*, 201(4914), 68-69.

Connolly, Kate (2015-06-08). "G7 leaders agree to phase out fossil fuel use by end of century". *The Guardian*. ISSN 0261-3077.

da Silva, G. L., Silva, R. D., Cheloni, L., de Souza Moreira, V. E., Dias Haneiko, N. B., & Assis, P. S. (2016). Characterization of Metallurgical Coke Produced with Coal Mixtures and Waste Tires. *Materials Research-Ibero-American Journal of Materials*, 19(3), 728–734.

Diaz-Faes, E., Barriocanal, C., Diez, M. A., & Alvarez, R. (2007). Applying TGA parameters in coke quality prediction models. *Journal of Analytical and Applied Pyrolysis*, 79(1-2 SPEC. ISS.), 154–160.

Diez, M. A., Alvarez, R., & Barriocanal, C. (2002). Coal for metallurgical coke production: Predictions of coke quality and future requirements for cokemaking. *International Journal of Coal Geology*, 50(1-4), 389–412.

Dombrovskii, V. P., Dyusembaev, D. E., & Ryaschchikov, V. I. (1988). Continuous determination of the ash content of coke in blast-furnace weigh hoppers. *Metallurgist*, 32(4), 137-139.

Fuertes, A., Pis, J., Pérez, A., Lorenzana, J., Pajares, J., & Palacios, J. (1989). Variation of the textural properties of a coke during gasification. *Vacuum*, 39(7-8), 677–681.

Gornostayev, S., Harkki, J., & Kerkkonen, O. (2009). Transformations of pyrite during formation of metallurgical coke. *Fuel*, 88(10), 2032–2036.

Grigore, M., Sakurovs, R., French, D., & Sahajwalla, V. (2006). Influence of Mineral Matter on Coke Reactivity with Carbon Dioxide. *ISIJ International*, 46(4), 503–512.

Grigore, M., Sakurovs, R., French, D., & Sahajwalla, V. (2012). Properties and CO₂ reactivity of the inert and reactive maceral-derived components in cokes. *International Journal of Coal Geology*, 98, 1–9.

Grosspietsch, K. H., & Lungen, H. B. (2000). Coke quality requirements by European blast furnace operators. In *Mezinarodni koksarenska konference*(pp. 31-39).

Gupta, S., French, D., Sakurovs, R., Grigore, M., Sun, H., Cham, T., Gupta S., Chandratilleke, R., & Sahajwalla, V. (2008). Minerals and iron-making reactions in blast furnaces. *Progress in Energy and Combustion Science*, 34(2), 155–197.

Hao, L. F., Ping, F. E. N. G., Song, W. L., Lin, W. G., Yoon, S. H., & Mochida, I. (2012). Modification performance of Hypercoal as an additive on co-carbonization of coal. *Journal of Fuel Chemistry and Technology*, 40(9), 1025-1030.

Harris, D. J., & Smith, I. W. (1989). Intrinsic Reactivity of Coke and Char to Carbon Dioxide, (1), 94–101.

Hays, D., Patrick, J. W., & Walker, A. (1976). Pore structure development during coal carbonization. 1. Behaviour of single coals. *Fuel*, 55(4), 297–302.

Hilding, T., Gupta, S., Sahajwalla, V., Björkman, B., & Wikström, J.-O. (2005). Degradation Behaviour of a High CSR Coke in an Experimental Blast Furnace: Effect of Carbon Structure and Alkali Reactions. *ISIJ International*, 45(7), 1041–1050.

IEA. (2016). Key World Energy Statistics 2016. Statistics, 80.

Inoue K., Masuda K., Okuyama N., Komatsu N., Hamaguchi S., Shinda R. (2008). Influence of Hyper-Coal addition on cokes pore distribution, The Japan Energy Society, pp. (130-131)

International Energy Agency. (2015). Key Coal Trends. IEA Report, 22.

Knoerzer, Jerome J., Cekela, Vincent W. Jewell-Thompson non-recovery cokemaking (1993) *Steel Times*, 221 (4), pp. 172-173, 184.

Kobayashi, H., Howard, J. B., & Sarofim, A. F. (1977, January). Coal devolatilization at high temperatures. In *Symposium (international) on combustion* (Vol. 16, No. 1, pp. 411-425).

Koszorek, A., Krzesińska, M., Pusz, S., Pilawa, B., & Kwiecińska, B. (2009). Relationship between the technical parameters of cokes produced from blends of three Polish coals of different coking ability. *International Journal of Coal Geology*, 77(3-4), 363–371.

Krzesińska, M., Pusz, S., & Smedowski, Ł. (2009). Characterization of the porous structure of cokes produced from the blends of three Polish bituminous coking coals. *International Journal of Coal Geology*, 78(2), 169–176.

Li, C., Yang, S., Chen, X., Lin, X., & Wang, Y. (2017). The characteristic of Shengli brown coal fractions from heavy medium separation and its influence on CO₂ gasification. *Fuel Processing Technology*, 155, 232–237.

- Loison, R., Foch, P., & Boyer, A. (1989). Coke quality criteria. *COKE Quality and Production*, 190.
- MacPhee, T., Giroux, L., Ng, K. W., Todoschuk, T., Conejeros, M., & Kolijn, C. (2013). Small scale determination of metallurgical coke CSR. *Fuel*, 114, 229–234.
- Mccandless, F. P., & Blake, J. M. (1970). Characterization of Asphalt for Use as Binder, 9(2), 183–186.
- Mennella, V., Monaco, G., Colangeli, L., & Bussoletti, E. (1995). Raman spectra of carbon-based materials excited at 1064 nm. *Carbon*, 33(2), 115-121.
- Mollah, M. M., Jackson, W. R., Marshall, M., & Chaffee, A. L. (2015). An attempt to produce blast furnace coke from Victorian brown coal. *Fuel*, 148, 104–111.
- Nag, D., Das, B., Dash, P. S., Sen, S., Paul, S., Verma, S., & Haldar, S. K. (2017). Use of phenolic resin in coke making at Tata Steel. *Ironmaking & Steelmaking*, 44(7), 526–531
- Nomura, S. (2016). Coal briquette carbonization in a slot-type coke oven. *Fuel*, 185, 649–655.
- Nomura, S. (2017). Recent developments in cokemaking technologies in Japan. *Fuel Processing Technology*, 159, 1–8.
- Okuhara, T., Nakama, H., & Miura, Y. (1981). Carbonization behaviour of coal briquettes in a slot-type coke oven. *Fuel*, 60(11), 1091–1095.
- Paul, S. A., Hull, A. S., Plancher, H., & Agarwal, P. K. (2002). Use of asphalts for formcoke briquettes. *Fuel Processing Technology*, 76(3), 211–230.

Peters, J. T., Schapiro, N., & Gray, R. J. (1962). *Know your coal*. Public Relations Department, United States Steel Corporation.

Rahman, M., Samanta, A., & Gupta, R. (2013). Production and characterization of ash-free coal from low-rank Canadian coal by solvent extraction. *Fuel processing technology*, 115, 88-98.

Rodero, J. I., Sancho-Gorostiaga, J., Ordiales, M., Fernandez-Gonzalez, D., Mochon, J., Ruiz-Bustanza, I., ... Verdeja, L. F. (2015). Blast Furnace and Metallurgical Coke's Reactivity and Its Determination by Thermal Gravimetric Analysis. *Ironmaking & Steelmaking*, 42(March), 1743281215Y.0000000016.

Sato, H., Patrick, J. W., & Walker, A. (1998). Effect of coal properties and porous structure on tensile strength of metallurgical coke. *Fuel*, 77(11), 1203–1208.

Saxena, V. K., & Tiwari, H. P. (2016). Coal to Metallurgical Coke, 363–382.

Sharma, M. K., Chaudhuri, a. J., Prasad, S., Prasad, B. N., Das, a. K., & Parthasarthy, L. (2007). Development of New Coal Blend Preparation Methodologies for Improvement in Coke Quality. *Coal Preparation*, 27(907688104), 57–77.

Sivanaskar (2008), *Engineering Chemistry*, 355-357

Takanohashi, T., Shishido, T., & Saito, I. (2008). Effects of hypercoal addition on coke strength and thermoplasticity of coal blends. *Energy and Fuels*, 22(3), 1779–1783.

Tiwari, H. P., Banerjee, P. K., & Saxena, V. K. (2013). A novel technique for assessing the coking potential of coals/coal blends for non-recovery coke making process. *Fuel*, 107, 615–622.

Trejo, F., Rana, M. S., & Ancheyta, J. (2010). Thermogravimetric determination of coke from asphaltenes, resins and sediments and coking kinetics of heavy crude asphaltenes. *Catalysis Today*, 150(3-4), 272–278.

Tupkary R. H. & Tupkary V.H. (2013). An Introduction to Modern Iron Making, 43-54

Urych, B. (2014). Determination of Kinetic Parameters of Coal Pyrolysis to Simulate the Process of Underground Coal Gasification (UCG). *Journal of Sustainable Mining*, 13(1), 3–9.

Veld Leon, (2006, May 23), “Review of the market for Metallurgical Coal”. Retrieved from <http://www.bhp.com/-/media/bhp/documents/investors/reports/2006/060523leondeveldmccloskeycoalconf.pdf>

Warren, W. M. B. (1938). Carbonization of Typical Bituminous Coals. *Industrial & Engineering Chemistry*, 30(2), 136-141.

Willmers, R. R. (1992). Coke properties in the bosh and raceway regions of the blast furnace. *Revue de Métallurgie*, 89(3), 241-250.

World Steel Association. (2011). Steel and Raw materials, 15(4), 710–739.

Wu, W. R. K.; Storch, H. H. (1968) "Hydrogenation of Coal and Tar", U. S. Department of the Interior, Bureau of Mines Bull. 633, 195 pp.

Xing, X., Zhang, G., Dell’Amico, M., Ciezki, G., Meng, Q., & Ostrovski, O. (2013). Effect of annealing on properties of carbonaceous materials. Part II: porosity and pore geometry. *Metallurgical and Materials Transactions B*, 44(4), 862-869.

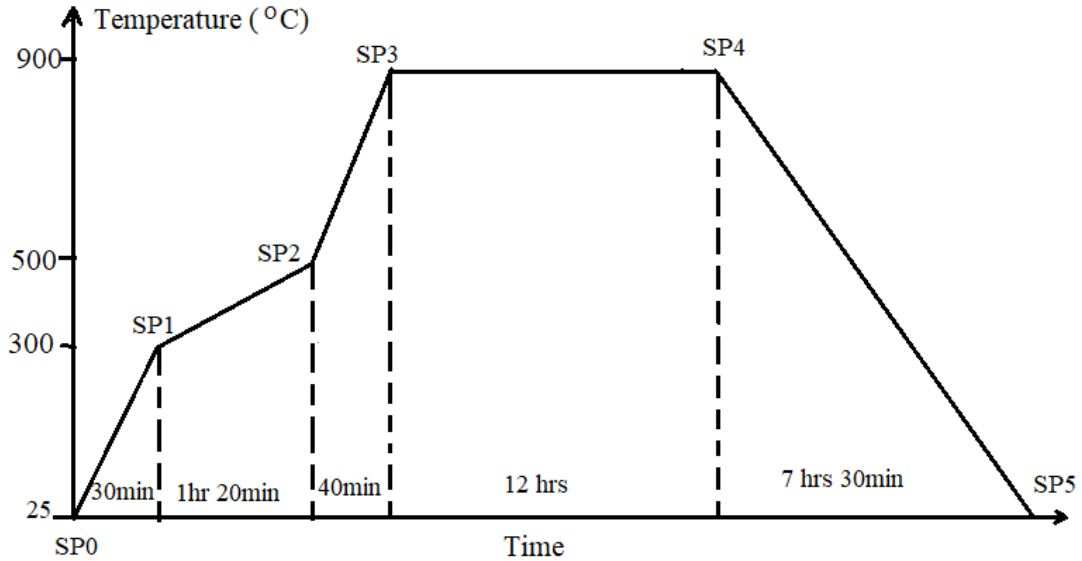
Ye, D. P., Agnew, J. B., & Zhang, D. K. (1998). Gasification of a South Australian low-rank coal with carbon dioxide and steam: kinetics and reactivity studies. *Fuel*, 77(11), 1209-1219.

Zhong, X., Wu, S., Liu, Y., Zhao, Z., Zhang, Y., Bai, J., Xi, B. (2013). Research on the evolvement of morphology of coking coal during the coking process. *Journal of Environmental Sciences (China)*, 25(S1), S186–S189.

APPENDICES

Operation of the horizontal tube furnace

The heating cycle for the carbonization process is illustrated below.



<i>Step</i>	<i>Set Point (SP)</i>	<i>Time (hr,min)</i>
<i>Step 0</i>	25	0,00
<i>Step 1</i>	300	0,30
<i>Step 2</i>	500	1,20
<i>Step 3</i>	900	0,40
<i>Step 4</i>	900	12,00
<i>Step 5</i>	25	7,30

The operating program was set in the furnace by the following steps.

The switch was turned on.

To select menu display,  was pressed for 2 seconds and Program mode, **PrGm** was selected using  or  keys.

The  key was pressed for 2 seconds to enter into program mode. Then, 'Ptrn' is displayed. Default id is set to "0".

The  key was pressed once and the display showed [S-no] number of steps.

The number of steps was set to '5' using  or  keys.

The  key was pressed and then, [SP0] showed. '25' was set for temperature using  or  keys.

The  key was pressed and then, [t 0] showed. 0:00 was set for time parameter.

The rest of the steps were input using the procedure no. 5 and 6 and then the  key was pressed again. The 'pattern execution count' parameter was displayed. Default was set as 1.

The rest of the parameters were set as [rpt]: as 1, alarm 1, [AL-1] was set at 950 to prevent heating beyond 950°C and [AL-2] was set at 0°C to prevent overcooling.

The  key was pressed for 2s to return to program mode until **PrGm** was displayed.

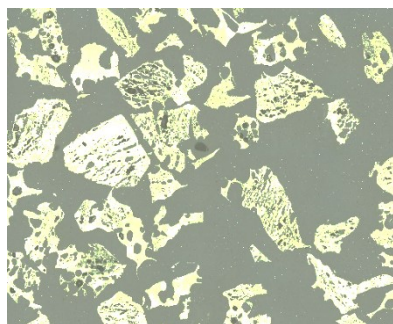
 or  keys was clicked to go to [Lu 0]

The  key was pressed for 2s to return to main page showing Set Point (SP) and Present Value (PV).

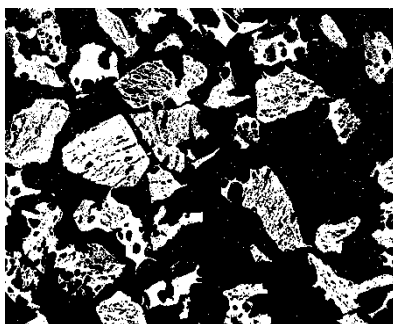
Finally, the RUN/RST button was pressed till the orange light above the  key turned off and the program starts working.

Steps of image processing to find total porosity of cokes

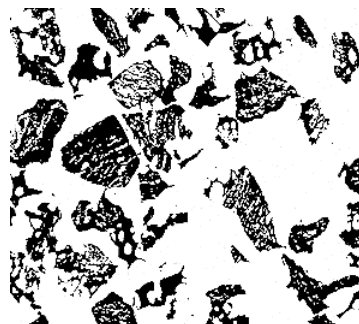
The image that was two-dimensionally stitched in microscope was subjected to image processing in MATLAB using two steps. At first, it was converted into a binary image by thresholding. The coke surfaces were kept white and the porosity was turned black. The total area of the coke surface was then calculated from this binary image. In the next step, the binary image was subjected to inverse of color to obtain the total area of the empty space.



Actual image



Thresholded image



Inversed image

Then total porosity of the coke was calculated using the formula

$$Porosity = 100 * A / (A + B)$$

Where,

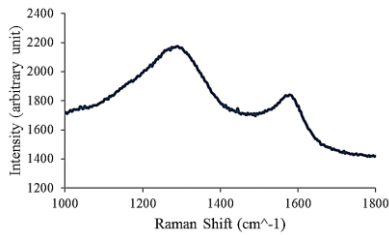
A = total surface area of the coke sample

B = total surface area of the pores.

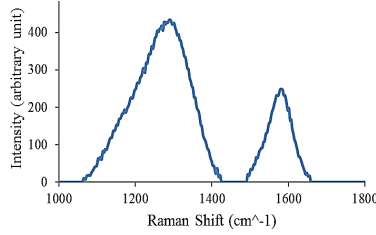
Steps of calculation for extent of graphitization

The obtained Raman spectrum lacked a proper horizontal baseline. Hence, the spectrum was subjected to baseline correction using the relevant function in OriginPro software. Then the area

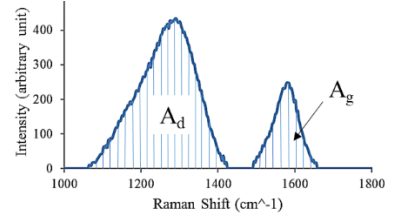
under the peaks were obtained using trapezoidal formula. The steps are summarised in the figure below.



Obtained Raman spectrum



Spectrum with corrected baseline



Area under the peaks calculated

The area under the peaks were broken down into small trapezoids and their individual area were calculated using the formula mentioned below. The total area was calculated using the summation of individual areas.

Area of each section:

$$\text{Trapezoid area} = \frac{(a+b)}{2} \times h$$

Where

a,b= parallel sides and h= height of trapezoid

$$\text{Area under peak} = \sum \text{Trapezoid Area}$$

Then the extent of graphitization was calculated using the following formula:

$$\frac{A_g}{A_g + A_d} \times 100 = \text{Extent of graphitization}$$

Where,

A_g = Area under G peak

A_d = Area under the D peak